Journal of Sustainable Development and Policy

Volume: 3; **Issue:** 3
Pages: 87-133

COMPUTATIONAL THERMO-FLUID DYNAMICS MODELING FOR PROCESS OPTIMIZATION IN HYDROGEN-INTEGRATED INDUSTRIAL HEAT SYSTEMS

Saikat Sarkar[1];

[1]. *Maintenance Engineer, Chemtrade Refinery Service Inc. Beaumont, Texas, USA; Email: saikat.mac@gmail.com*

Doi: 10.63125/8rm6bc88
Received: *18 July 2024;* ***Revised:*** *17 August 2024****; Accepted: 17*** *September 2024****; Published:*** *28 September 2024*

Abstract

This study evaluated computational thermo-fluid dynamics modeling as a quantitative platform for process optimization in hydrogen-integrated industrial heat systems. A validated three-dimensional reacting CFD model was executed as a controlled numerical experiment across 60 design-of-experiments cases that spanned hydrogen volumetric shares from 0% to 100% (mean 52.3%, SD 30.1), oxidizer staging ratios from 0.50 to 0.90 (mean 0.70), swirl/mixing levels from 0.20 to 0.90 (mean 0.56), jet momentum ratios from 0.60 to 1.80 (mean 1.12), and recirculation rates from 0% to 25% (mean 11.8%). Extracted responses showed practical but non-uniform hydrogen effects: useful heat-transfer efficiency ranged from 71.2% to 86.5% (mean 79.8%, SD 4.1), load temperature spread increased markedly from 18.4°C to 72.9°C (mean 41.6°C, SD 13.8), peak wall temperature varied between 1125°C and 1328°C (mean 1224°C), chamber pressure drop rose from 185 to 412 Pa (mean 298 Pa), and NOx emission index spanned 0.38 to 1.54 g/MJ (mean 0.92 g/MJ). Correlation screening indicated strong positive associations between hydrogen share and NOx (r = 0.61), peak wall temperature (r = 0.52), and temperature spread (r = 0.47), while the link to efficiency was weak (r = 0.18). Reliability checks showed repeatability differences below 3% for all indicators and medium–fine mesh differences below 3.1%, confirming numerical stability. Multivariate regressions revealed that hydrogen share significantly increased NOx, wall hot spots, non-uniformity, and pressure drop, whereas oxidizer staging and swirl significantly mitigated these penalties; the hydrogen–staging interaction produced the largest NOx suppression. Feasible operating windows were therefore characterized by moderate-to-high hydrogen shares combined with elevated staging and swirl, preserving efficiency while meeting emissions, stability, pressure-loss, and material-temperature constraints.

Keywords

Hydrogen combustion, Thermo-fluid CFD, Process optimization, Industrial heat, NOx control.

INTRODUCTION

Computational thermo-fluid dynamics modeling is the systematic numerical representation of interacting heat-transfer and fluid-flow phenomena in engineered systems, typically expressed through the conservation laws of mass, momentum, energy, and chemical species (Deutschmann, 2015). In industrial contexts, this modeling family includes steady and transient simulations of convection, conduction, radiation, buoyancy, turbulence, compressibility, multiphase transport, and reactive flow, all solved on discretized domains that mimic real equipment geometries. The term "process optimization" denotes a quantitative effort to adjust design variables and operating conditions so that predefined performance objectives are maximized or minimized under explicit constraints. In industrial heat systems, those objectives often include thermal efficiency, heat-flux uniformity, product quality stability, throughput, fuel utilization, and emissions control, while constraints include burner stability limits, safety thresholds, refractory durability, allowable pressure drops, and production schedules. Hydrogen-integrated industrial heat systems are high- or medium-temperature process-heat assets that introduce hydrogen as a fuel, co-fuel, or heat carrier within established thermal architectures such as furnaces, kilns, boilers, reformers, heaters, and heat-recovery networks (Adair & Jaeger, 2019). International significance follows from the scale and hardness of industrial heat demand. Heavy industries represent a substantial fraction of global final energy use, and their process heat is frequently required at temperatures that challenge direct electrification. Across multiple world regions, decarbonization roadmaps identify hydrogen as a promising option for medium-to-high temperature heat because hydrogen combustion produces no carbon dioxide at the point of use and can be deployed through retrofits rather than full asset replacement. Parallel interest comes from energy security concerns, diversification of fuel portfolios, and the need to maintain competitive production costs under tightening environmental standards. Yet hydrogen changes the internal thermo-fluid behavior of heat systems in ways that are not captured by simple energy-balance calculations. The introduction of hydrogen influences flame structure, thermal radiation, convective mixing, density-driven circulation, and pollutant pathways. These influences are strongly coupled, spatially heterogeneous, and equipment-specific, which explains why computational thermo-fluid modeling has become central to the quantitative assessment and optimization of hydrogen-integrated heat processes (Casella, 2017). Multiple experimental and numerical studies across diverse industrial sectors collectively show that reliable predictive modeling is essential for scaling hydrogen use from pilot trials to internationally relevant production operations, because it provides controlled access to the flow and temperature fields that drive performance outcomes.

Hydrogen's physical, transport, and combustion characteristics define the distinctive thermo-fluid problem posed by hydrogen-integrated industrial heat systems. Relative to typical hydrocarbon fuels, hydrogen exhibits very low molecular weight, high diffusivity, a broad flammability range, low ignition energy, and high laminar flame speed (Chen et al., 2017). These properties increase the sensitivity of combustion to mixing patterns and local strain rates, producing flame behaviors that shift with burner momentum, swirl, staging, and oxygen availability. In practical furnaces, hydrogen enrichment changes jet penetration, entrainment, and recirculation zones, which in turn reshapes where heat is released and how it reaches the load. Hydrogen flames also alter the balance between radiative and convective heat transfer. Without soot formation, hydrogen flames in air are generally less luminous, so direct flame radiation to walls and products can decrease, while convective transfer and wall re-radiation can become relatively more important. In oxy-fuel or oxygen-enriched firing, the radiating species field changes substantially because the combustion products are dominated by water vapor with minimal carbon dioxide, shifting spectral emission characteristics and thus total radiative heat flux. These effects influence temperature uniformity, refractory wear patterns, and load heating rates (Papasidero et al., 2017). Another well-documented aspect is pollutant formation: hydrogen combustion can elevate thermal nitrogen oxides when peak temperatures and oxygen availability align in localized zones, so burner and staging adjustments are needed to maintain emissions compliance. At the same time, hydrogen's high volumetric flow demand for equal thermal input affects pressure losses and fan or blower requirements, shaping furnace aerodynamics at scale. Findings from many sector-specific trials show that small changes in hydrogen ratio can produce non-linear changes in stability, heat-flux distribution, and emissions. Because these outcomes arise from coupled thermo-

fluid processes rather than from fuel chemistry alone, numerical modeling that resolves flow, heat transfer, and reaction together is required to interpret hydrogen's role. Computational thermo-fluid dynamics therefore serves as a bridge between hydrogen property fundamentals and performance-critical industrial behavior, enabling quantitative comparison across burner types, furnace geometries, and operating regimes found in different countries and industrial traditions (Rzehak, 2016).

Figure 1: Hydrogen-Integrated Thermo-Fluid Process Optimization

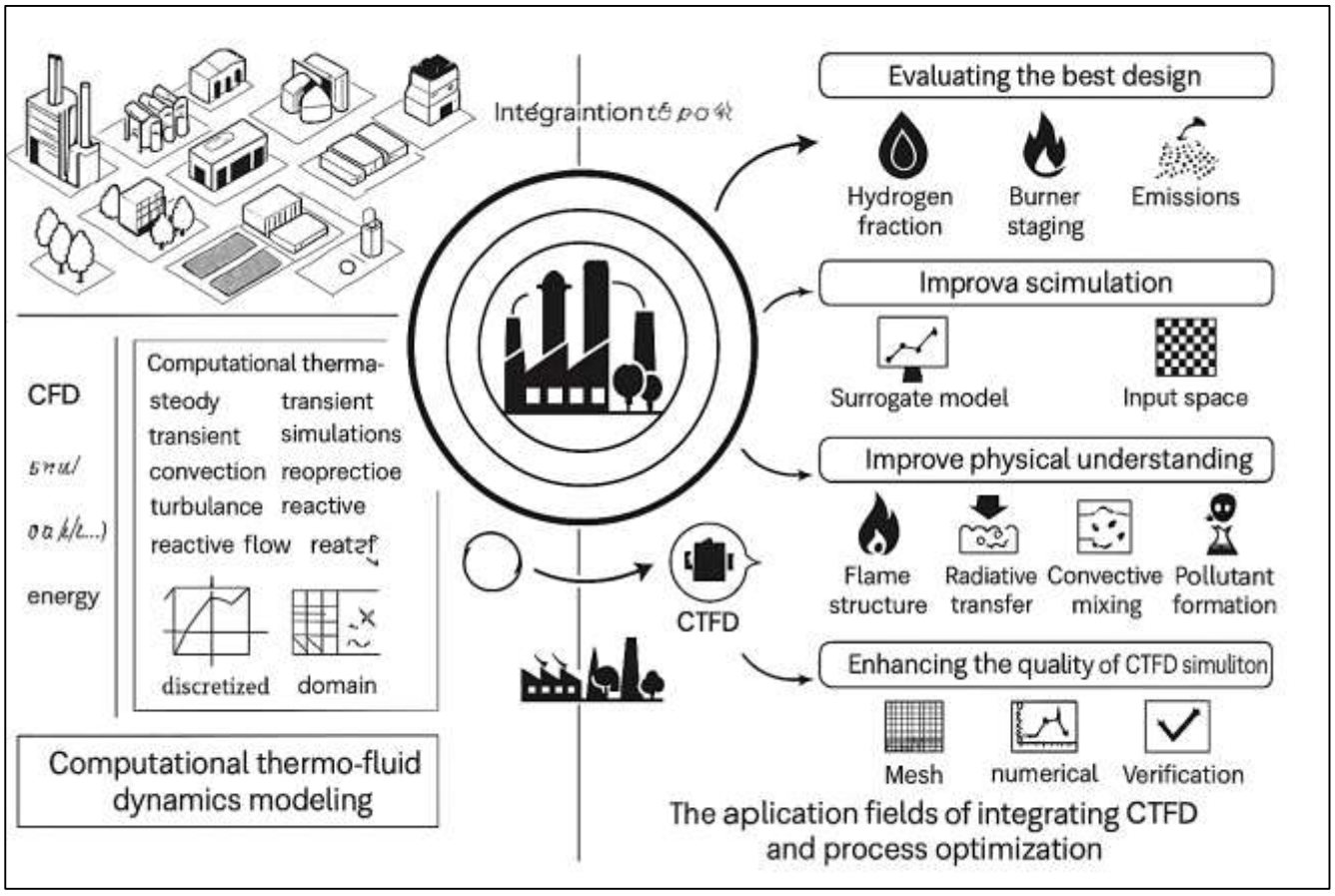

The mathematical and numerical structure of computational thermo-fluid dynamics modeling provides the basis for prediction and optimization. At its core, industrial reacting-flow CFD solves discretized forms of the Navier–Stokes equations coupled to energy conservation and species transport. The energy equation includes enthalpy convection, conductive diffusion, volumetric heat release from reactions, and radiative source terms (Arfan et al., 2021; Introini et al., 2018). Species equations include multi-component diffusion and chemical source terms that represent hydrogen oxidation pathways. Turbulence closure is a central modeling decision because industrial heat systems are dominated by high-Reynolds-number flows with swirl, buoyancy, and heavy recirculation. Design-level simulations often use Reynolds-averaged turbulence models to approximate mean flow and turbulent transport, while more detailed studies use scale-resolving approaches to capture coherent structures that influence flame wrinkling and heat transfer (Jahid, 2021; Akbar & Farzana, 2021). Combustion sub-models determine how turbulence and chemistry interact. Industrial hydrogen studies have applied mixing-limited approaches, finite-rate chemistry with turbulence interaction, flamelet-based manifolds, transported probability density frameworks, and thickened or adaptive flame models, each chosen according to regime, computational cost, and required fidelity. Radiation modeling is equally indispensable in high-temperature equipment (Guelpa et al., 2016; Reza et al., 2021; Saikat, 2021). Participating-media radiation is modeled through angular discretization or diffusion-type approximations, combined with spectral band methods that capture water-vapor dominated emission (Shaikh & Aditya, 2021; Kanti & Shaikat, 2021). Conjugate heat transfer links gas-side fields to solid refractories, metallic walls, or moving loads, ensuring that wall temperatures and heat losses are

predicted consistently. Industrial geometries require robust meshing strategies that balance resolution near burners and heat-transfer surfaces with manageable cell counts across large enclosures (Zobayer, 2021a, 2021b). Transient integration is important where burner cycling, load movement, regenerative switching, or hydrogen ratio modulation alter boundary conditions over time. Verification and validation practices, widely documented in the modeling literature, connect numerical predictions to plant measurements such as flue-gas temperatures, wall thermocouples, heat-flux probes, exhaust composition, and pressure drops (Ariful & Ara, 2022; Arman & Kamrul, 2022). These practices help quantify discretization error, model-form uncertainty, and parameter sensitivity. In hydrogen-integrated heat systems, such rigor is magnified because hydrogen can steepen gradients near injectors and intensify turbulence-chemistry coupling (Liu et al., 2016; Mesbaul & Farabe, 2022). For optimization, this predictive foundation allows the conversion of simulated field quantities into measurable performance indicators, providing the quantitative substrate on which improved operating policies and design modifications can be evaluated systematically (Nahid, 2022; Hossain & Milon, 2022).

Hydrogen integration has been investigated across multiple heat-intensive industrial sectors, each adding distinctive thermo-fluid constraints that computational modeling can resolve (Abdur & Haider, 2022; Mushfequr & Praveen, 2022). In steel reheating furnaces, hydrogen substitution affects flame impingement, recirculation, and billet heating uniformity, with consequences for metallurgical quality, scale formation, and fuel economy (Ayr et al., 2015; Mortuza & Rauf, 2022; Rakibul & Samia, 2022). Steel trials and simulations report that hydrogen alters near-burner temperature peaks and wall heat flux patterns, requiring burner staging and momentum tuning to retain uniform product temperatures (Rony & Ashraful, 2022; Saikat, 2022). In cement production, hydrogen blending in kiln and calciner burners changes the gas-solid heat transfer field that governs calcination and clinker formation. The long, rotating kiln geometry produces axial temperature gradients and complex recirculation zones, so thermo-fluid modeling is used to evaluate how hydrogen modifies residence times, radiative exchange, and local oxygen levels important for stable operation (Abdul, 2023; Abdulla & Zaman, 2023). Glass melting furnaces rely heavily on radiative transfer for melt heating; hydrogen's altered radiance changes crown heat flux, melt-surface temperature distributions, and convective circulation above the melt, so multi-radiation CFD is needed to avoid cold regions or excessive refractory loading (Arfan et al., 2023; Di Martino et al., 2019). Petrochemical cracking furnaces and reformer fireboxes involve dense tube banks where radiative and convective transfer to coils must be controlled to prevent tube overheating and coking. Hydrogen firing influences flame shape and gas emissivity, shifting coil heat rates and tube metal temperature profiles, which modeling can map at high spatial resolution (Amin & Mesbaul, 2023; Foysal & Aditya, 2023). In boiler-based sectors such as pulp and paper or food processing, hydrogen blending interacts with low-NOx burner designs and flue-gas recirculation loops, affecting flame stability, heat-exchanger approach temperatures, and stack emissions (Hamidur, 2023; Rashid et al., 2023). Across these sectors, studies comparing different hydrogen ratios indicate that equipment-specific flow structures mediate the net thermal effect, meaning outcomes cannot be generalized from fuel properties alone. International industrial diversity further reinforces this point (Musfiqur & Kamrul, 2023; Muzahidul & Mohaiminul, 2023): furnace sizes, air or oxygen supply practices, refractory materials, and emission standards differ across regions, so predictive modeling is essential for transferring hydrogen insights between installations (Bugatti & Semeraro, 2018; Amin & Sai Praveen, 2023; Hasan & Ashraful, 2023). By recreating full-scale enclosure aerodynamics and heat-transfer pathways, computational thermo-fluid dynamics supports sector-specific optimization hypotheses in a way that experimental campaigns alone cannot, establishing a shared quantitative language for hydrogen integration in globally distributed process-heat applications.

Industrial heat systems operate as networks rather than isolated devices, and computational thermo-fluid modeling increasingly includes auxiliary components that shape overall performance under hydrogen integration (Mushfequr & Ashraful, 2023; Roy & Kamrul, 2023). Many plants combine radiant chambers, convection passes, recuperators, regenerators, and waste-heat boilers into tightly coupled heat-recovery ecosystems (Kabeel et al., 2019). Hydrogen alters flue-gas composition and thermophysical properties, influencing density, viscosity, specific heat, and radiative behavior, which collectively change convective heat-transfer coefficients and temperature driving forces in downstream

exchangers (Saba et al., 2023; Saba & Kanti, 2023). Modeling studies of waste-heat recovery devices show that flow maldistribution, bypassing, and fouling can reduce recovery efficiency, and these effects are sensitive to fuel-dependent exhaust characteristics. When hydrogen shares increase, volumetric exhaust flows and moisture content often rise, requiring reevaluation of exchanger pressure drops and heat-transfer surfaces (Shaikh & Farabe, 2023; Haider & Hozyfa, 2023). Thermal energy storage adds another coupling layer, including packed beds, molten salts, or phase-change materials that buffer intermittent hydrogen supply or enable load shifting (Zheng et al., 2016; Zobayer, 2023). CFD-based investigations of thermal storage demonstrate that transient convection patterns, stratification, and melt-front movement largely determine effective storage capacity and charge-discharge efficiency (Abdul & Shoeb, 2024). In hydrogen-integrated plants, storage behavior intersects with burner scheduling, oxygen staging, and heat-recovery train setpoints, which motivates integrated simulations (Hozyfa & Shahrin, 2024; Jabed Hasan & Shah, 2024). Hybrid modeling frameworks link device-scale CFD zones to plant-scale models of fuel preparation, compression, storage, and distribution manifolds, allowing process heat simulations to reflect real supply constraints and dynamic operating envelopes (Hasan & Zayadul, 2024; Muzahidul & Aditya, 2024). Digital twin applications for high-temperature units embed thermo-fluid solvers within live process representations, enabling recalculated temperature and flow fields as boundary conditions change during hydrogen blending tests. Such coupling is central for optimization because improvements at burner or furnace level may interact with recovery loop performance or storage dispatch decisions (Hasan & Rakibul, 2024; Mominul, 2024). Multiple studies show that a full-system view can reveal tradeoffs between peak-zone control in radiant spaces and overall heat-recovery efficiency, especially under varying hydrogen input (Mominul & Zaki, 2024; Roy & Sai Praveen, 2024). Computational thermo-fluid dynamics offers the only scalable way to represent these cross-component interactions at the required spatial and temporal fidelity, providing unified quantitative evidence for optimizing hydrogen-integrated heat systems as coherent industrial networks (Qu et al., 2019; Rahman et al., 2024; Rony & Hozyfa, 2024).

Figure 2: Hydrogen Thermo-Fluid Optimization Framework

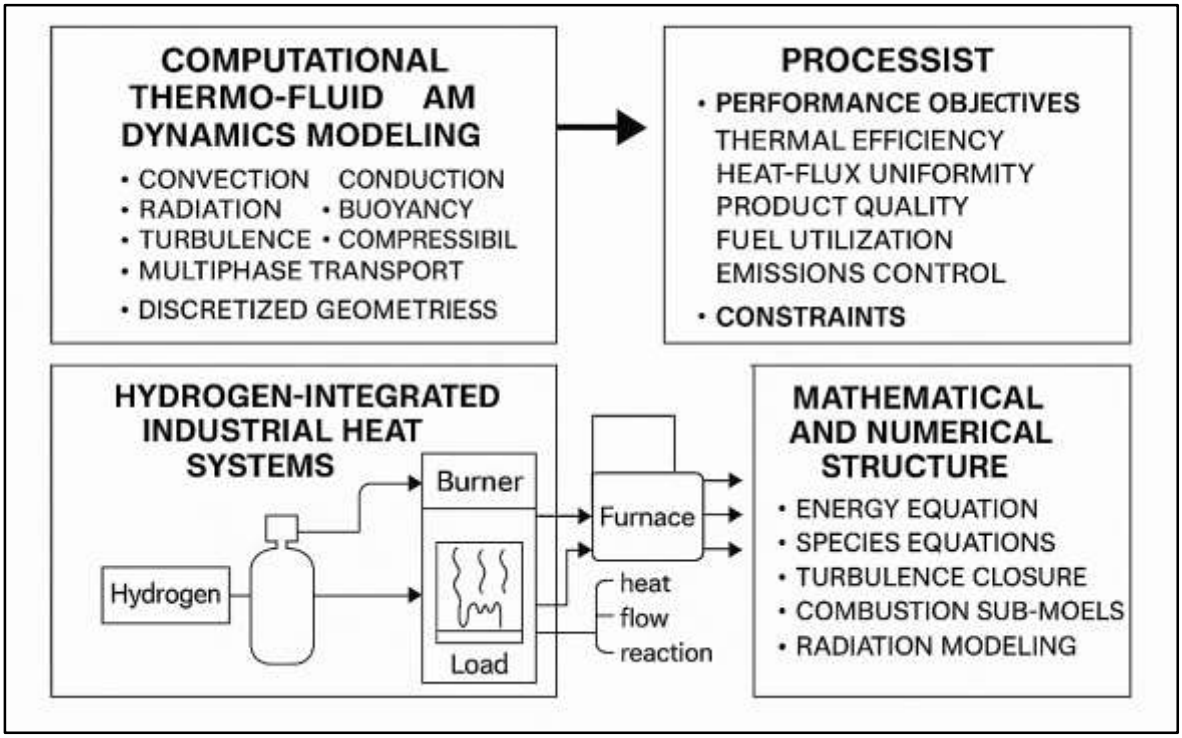

Optimization methods built on computational thermo-fluid dynamics convert simulated field data into structured decision support for design and operation (Saba & Hasan, 2024; Shaikat & Zaman, 2024). A common quantitative approach is to define objective functions such as total useful heat to the load, mean and variance of load temperature, fuel-to-heat efficiency, maximum wall temperature, and

emission indices for nitrogen oxides, carbon monoxide, or unburned hydrogen (Chang & Dinh, 2019). Decision variables include hydrogen fraction, burner equivalence ratio, air staging splits, swirl intensity, jet momentum ratios, injector locations, recirculation rates, and furnace pressure setpoints. Many studies have used design-of-experiments and response surface methods to explore these variables efficiently, fitting surrogate models that approximate CFD outputs across a multidimensional design space. Kriging and other Gaussian-process surrogates are applied where response surfaces are complex or noisy, enabling rapid evaluation of candidate settings. Multi-objective optimization is frequently required because thermal efficiency and emissions constraints compete, and Pareto-front analyses allow identification of balanced operating regions. Evolutionary algorithms are used when objective landscapes are non-convex or discontinuous due to ignition thresholds or stability boundaries. Gradient-based methods, including adjoint sensitivity techniques, are employed where smooth dependencies permit efficient navigation toward optimal shapes or boundary conditions (Lamnatou et al., 2015). Machine learning has also been paired with CFD to reduce model order, accelerate thermal radiation prediction, or infer optimal control policies from large simulation datasets. Calibration strategies play a critical role: optimization outputs depend on reliable sub-models for turbulence-chemistry interaction, wall emissivity, and inlet distributions, so multiple studies prescribe iterative tuning against experimental or plant data followed by uncertainty propagation to ensure that optimized solutions remain robust within error bounds. In hydrogen-integrated heat systems, this optimization machinery is especially valuable because hydrogen affects stability and emissions in ways that can flip quickly with small parameter changes (Sudipto & Hasan, 2024; Kanti & Saba, 2024). Simulations reveal local hot spots, backflow risks, or oxygen-rich pockets that are difficult to observe directly but are decisive for constraint handling in optimization. By iterating CFD predictions with statistical or algorithmic search, industrial researchers have demonstrated systematic pathways to identify operating conditions that maintain stable hydrogen combustion, uniform heat delivery, and compliant emissions across a variety of equipment types and sector demands (Chen et al., 2019; Kanti & Praveen, 2024; Haider & Praveen, 2024). These methodological patterns establish the quantitative foundation for studying process optimization through computational thermo-fluid dynamics in hydrogen-integrated industrial heat systems (Zobayer & Kumar, 2024; Zulqarnain & Zayadul, 2024).

The objective of the present quantitative study is to develop and apply a high-fidelity computational thermo-fluid dynamics modeling framework that can predict, compare, and optimize the thermal, aerodynamic, and combustion performance of hydrogen-integrated industrial heat systems under realistic operating constraints. At the core, the study aims to resolve the coupled transport of momentum, heat, and reacting species in representative industrial enclosures—such as furnaces, boilers, kilns, and reformer fireboxes—where hydrogen is introduced as a fuel or co-fuel, and to translate these resolved fields into measurable performance indicators for optimization. Specifically, the objectives include: (1) constructing validated multiphysics CFD models that incorporate turbulence, hydrogen combustion kinetics, participating-media radiation dominated by water-vapor products, and conjugate heat transfer with refractory and load materials, so that temperature distribution, heat-flux pathways, pressure losses, and stability margins can be predicted with quantified numerical consistency; (2) characterizing how hydrogen fraction, burner momentum ratios, swirl intensity, air or oxygen staging, and flue-gas recirculation alter flame anchoring, recirculation zones, and radiative–convective heat transfer balance, thereby determining product or load heating uniformity and peak wall temperatures; (3) computing emissions-relevant outcomes such as thermal nitrogen oxide propensity and residual unburned species indices as emergent results of local thermo-fluid conditions, enabling constraint-aware evaluation of hydrogen integration strategies; (4) coupling CFD outputs to optimization routines by defining objective functions that represent industrial priorities—useful heat to the load, thermal efficiency, temperature uniformity quantified via spatial variance, and emission indices—while enforcing safety and equipment constraints such as allowable wall temperature limits, minimum stability thresholds, and maximum pressure drops; (5) generating surrogate models from CFD datasets to accelerate parametric exploration and facilitate multi-objective search for optimal operating windows across hydrogen blending levels; and (6) producing a comparative optimization map that identifies the combinations of hydrogen share and combustion-aerodynamic settings that yield best-performing tradeoffs between efficiency, uniform heating, and emissions compliance for the

modeled system class. Collectively, these objectives position computational thermo-fluid dynamics not merely as a descriptive tool but as a quantitative optimization engine that can guide hydrogen integration decisions through physics-resolved prediction and systematic search over controllable process variables.

LITERATURE REVIEW

The literature on computational thermo-fluid dynamics modeling for industrial heat systems has expanded rapidly as industries evaluate hydrogen integration for high-temperature process heat (Zhao et al., 2019). This body of work spans three tightly connected domains: (a) the fundamental thermo-fluid and combustion behavior of hydrogen in turbulent industrial environments, (b) the numerical and multiphysics modeling strategies used to represent those behaviors in realistic furnaces, boilers, kilns, heaters, and heat-recovery units, and (c) the optimization methods that convert simulated flow and temperature fields into measurable improvements in efficiency, uniformity, stability, and emissions compliance. A literature review for this study therefore must do more than summarize general CFD progress; it must synthesize how hydrogen changes the governing physics of process heat, how these changes are captured or missed by existing computational approaches, and how simulation outputs have been quantitatively transformed into objective functions and constraint sets for optimization (Pettinau et al., 2015). Because hydrogen introduction modifies flame aerodynamics, heat-transfer mode balance, and pollutant formation through coupled mechanisms, prior studies vary significantly in turbulence–chemistry interaction models, radiative transfer treatment, boundary condition realism, and validation rigor. At the same time, process optimization studies differ in decision-variable selection, surrogate construction, and multi-objective tradeoff handling. This review is organized to trace a coherent chain from hydrogen-specific thermo-fluid fundamentals to industrial-scale numerical representation, and from representation to optimization, highlighting what has been quantified, how it has been quantified, and where methodological gaps remain in linking physics-resolved modeling with robust process-level optimization in hydrogen-integrated heat systems (Stamatakis et al., 2018).

Hydrogen-Integrated Industrial Heat Systems

Hydrogen-integrated industrial heat systems have emerged as a distinct class of thermal infrastructure within the broader taxonomy of process-heat technologies used in heavy industry. Industrial heat systems are purpose-built enclosures or networks that supply controlled thermal energy for material transformation, phase change, or high-temperature reaction work (Leblebici et al., 2018). The literature commonly differentiates these systems by geometry, dominant mode of heat transfer, and the nature of the heated load. Furnaces represent enclosed high-temperature units in which products such as steel billets, slabs, ceramics, or chemical intermediates are heated through direct or indirect flame interaction; subtypes include reheating furnaces for plastic deformation preparation, annealing furnaces for microstructural control, and heat-treatment furnaces for hardness and stress-relief management. Kilns, particularly rotary and shaft variants, are elongated reactors that combine continuous flow of solids with counter- or co-current hot gas for calcination or sintering, with cement, lime, and mineral processing as primary applications. Boilers and process heaters supply steam or hot air to downstream unit operations, typically featuring a combination of radiant firebox regions and convection passes. Reformer fireboxes and cracking furnaces are specialized petrochemical heaters where radiant heat transfer to tube banks governs endothermic reaction rates and product selectivity, making wall heat flux and tube metal temperature critical constraints (Vogel, 2019). Glass melters and float-glass furnaces rely on intense radiative heating of molten baths, with crown temperature management and melt homogeneity as principal performance targets. Across these categories, a recurring classification is the distinction between radiant-dominant chambers—where high-temperature flames and refractory surfaces deliver most heat by radiation—and convection-dominant chambers—where forced flow and heat-exchanger surfaces govern energy delivery. This distinction anchors much of the quantitative modeling work because it determines which physical sub-processes control efficiency, uniformity, and equipment life. Radiant-dominant systems emphasize volumetric heat release distribution, gas emissivity, surface emissivity, and view-factor geometry, while convection-dominant systems emphasize turbulent mixing, flow maldistribution, and convective coefficients at surfaces (Fulekar & Pathak, 2017). Several industrial case studies across steel, glass,

cement, and petrochemicals show that the same fuel change can yield different thermal outcomes depending on whether radiation or convection is the leading transfer pathway. Consequently, hydrogen integration is consistently framed not as a uniform substitution problem but as a system-specific transformation that must be evaluated against the operational logic of each heat-system type.

Hydrogen integration pathways in industrial heat systems are described in the literature through a small set of practical deployment modes that reflect existing burner technologies, fuel logistics, and safety requirements. Pure hydrogen firing involves replacing hydrocarbon fuels with hydrogen in compatible burners or newly installed hydrogen-ready hardware (Evangelopoulou et al., 2019). In this pathway, hydrogen becomes the sole chemical energy carrier, and performance is governed by hydrogen's transport behavior, combustion kinetics, and exhaust composition. Hydrogen–natural gas blends represent a transitional and widely studied route in which hydrogen is co-fed through existing fuel trains, sometimes with retrofitted nozzles or modified mixing zones to preserve flame anchoring and pressure balance. Blending ratios are commonly expressed in volumetric share and energy share because hydrogen's low volumetric energy density makes these two descriptors diverge meaningfully in practice; multiple industrial trials note that modest volumetric shares can represent small energy fractions, while high energy fractions may require large volumetric flow adjustments that reshape jet momentum and entrainment. Hydrogen-assisted oxy-fuel firing is a third pathway in which hydrogen is introduced under oxygen-rich or oxygen-only oxidizer environments, often to intensify radiative heat flux and reduce exhaust dilution (Ikäheimo et al., 2018). Studies of oxy-fuel retrofits highlight that hydrogen changes the radiative spectrum of combustion products by shifting the exhaust toward water-vapor dominance, which affects furnace heat transfer differently than both air-firing and hydrocarbon oxy-fuel cases. A fourth pathway uses hydrogen as a combustion enhancer rather than the primary fuel, where limited hydrogen addition improves flame stability, extends turndown ratios, or supports low-emission regimes through altered ignition and mixing characteristics. In these deployments, hydrogen acts as an operational lever for maintaining stable burning in staged or diluted flows. Industrial investigations consistently emphasize that pathway choice interacts with burner architecture, oxidizer supply constraints, and process atmosphere requirements. For example, furnaces requiring strongly reducing atmospheres must manage hydrogen addition differently than kilns operating under oxidizing conditions, while glass melters weigh oxy-fuel hydrogen benefits against crown temperature limits. Across at least a decade of trials and numerical analyses, the literature converges on the observation that hydrogen pathways cannot be summarized by fuel substitution alone; they are characterized by coupled changes in volumetric flow demand, stoichiometric operating windows, flame luminosity, and safety margins (Eveloy & Gebreegziabher, 2018). The pathway framework therefore provides an essential conceptual base for quantitative modeling and optimization because each pathway implies a different set of boundary conditions, controllable variables, and feasible operating ranges within industrial heat systems.

Quantitative performance indicators provide the measurement structure through which hydrogen-integrated industrial heat systems are assessed and compared. Thermal efficiency remains the most commonly used indicator, but studies treat it in multiple forms: overall system efficiency based on useful heat absorbed by the load relative to fuel input, combustion efficiency tied to unburned species, and heat-recovery efficiency linked to recuperators or regenerators (Rosen & Koohi-Fayegh, 2016). Heat-flux uniformity is another high-priority metric, operationalized through spatial or temporal dispersion of load temperature, wall heat flux, or product exit temperature. Steel reheating and heat-treatment research repeatedly shows that even small increases in temperature variance can produce microstructural inconsistency or yield losses, so uniformity indicators are treated as co-equal to efficiency in optimization. Peak wall or refractory temperature constraints form a third indicator family, because refractory wear, slagging risk, and tube-metal deterioration increase sharply with localized overheating. Across furnace and firebox studies, hydrogen introduction is observed to shift flame stabilization zones and convective circulation, which may move hot spots even when average temperatures remain stable. Pressure drop and fan power penalties are also embedded as quantitative constraints, especially for convective passes or high-recirculation burners, since hydrogen's volumetric demand can increase flow rates, altering aerodynamic losses (Speirs et al., 2018). Emissions indices extend performance evaluation into environmental compliance, with nitrogen oxides, carbon

monoxide, and residual unburned hydrogen reported per unit of useful energy or per unit of product output. Industrial burner and furnace case studies show that emissions respond to localized thermo-fluid conditions rather than to bulk fuel composition alone, so emission indices are interpreted alongside temperature and mixing fields. Operational stability margins form the final indicator group, incorporating quantitative proxies for blowoff and flashback risk, flame lift-off length, oscillation amplitude, or minimum stable equivalence ratios. Hydrogen's high flame speed and diffusion rate make stability a central concern across demonstration projects, and stability indicators are often treated as hard constraints in optimization rather than secondary outcomes. Across multiple sectors, comparative studies indicate that no single indicator adequately captures hydrogen integration performance in isolation; rather, the interplay between efficiency, uniformity, hot-spot control, aerodynamic cost, emissions, and stability defines the operational acceptability of hydrogen pathways (Felseghi et al., 2019). The literature therefore positions optimization as a multi-indicator problem, requiring model outputs mapped onto a structured performance set so that tradeoffs can be quantified consistently across equipment types and operating regimes.

Figure 3: Hydrogen Heat Systems Integration Framework

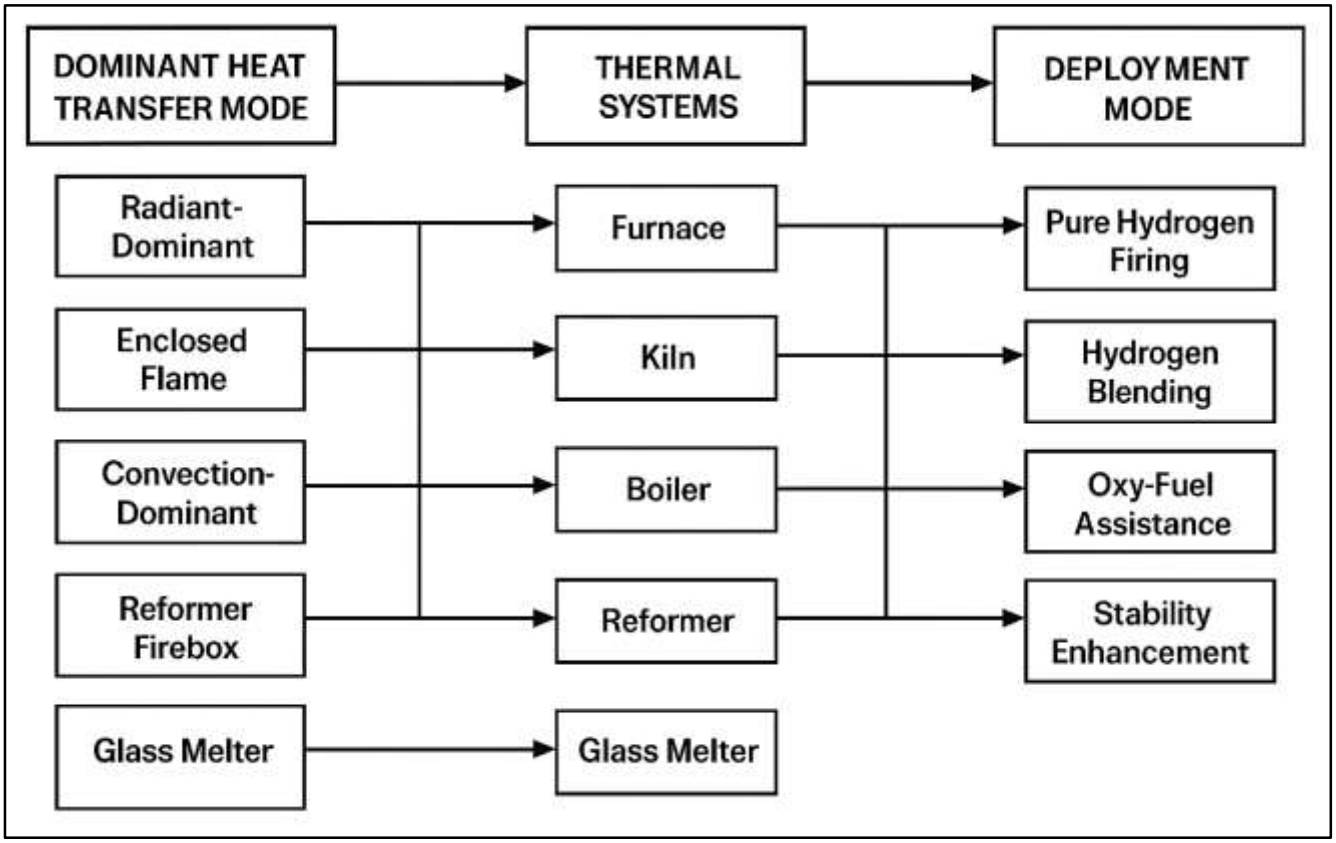

Taken together, the conceptual foundations of hydrogen-integrated industrial heat systems establish a quantitative frame that is directly compatible with computational thermo-fluid dynamics modeling. By defining the system class through furnace, kiln, boiler, reformer, cracking heater, and glass melter archetypes, prior work clarifies that hydrogen integration unfolds across a heterogeneous technical landscape where geometry and dominant heat-transfer mode determine outcome sensitivity (Cinti et al., 2019). Radiant-dominant systems foreground gas emissivity, surface radiation exchange, and heat-release positioning, while convection-dominant systems foreground turbulent transport, jet momentum control, and exchanger effectiveness. Hydrogen pathway definitions further translate this landscape into implementable deployment modes—pure firing, blending, oxy-fuel assistance, and stability-oriented enhancement—each implying different operational degrees of freedom and constraints. The performance indicator set then functions as a common language connecting hydrogen physics to industrial objectives, and it is this set that enables cross-study comparability in quantitative

literature. A consistent narrative across experimental trials, pilot retrofits, and numerical investigations indicates that hydrogen alters internal thermo-fluid fields in ways that redistribute radiative and convective heat delivery, change hot-spot topology, and reshape emission-formation regions. These effects manifest differently in steel reheating furnaces than in cement kilns, differently in glass melters than in petrochemical fireboxes, and differently again in boiler convection passes, largely because each system's thermal logic is distinct (Li et al., 2018). The literature also shows that optimization targets are rarely singular; high efficiency without uniformity control can degrade product quality, low emissions without stability margins can reduce operability, and improved heat recovery without aerodynamic feasibility can increase parasitic energy losses. Consequently, the conceptual groundwork developed across many studies supports a modeling-to-optimization chain in which computational thermo-fluid dynamics predicts coupled fields under hydrogen pathways, and those predictions are evaluated through standardized performance indicators. This grounding is essential for any quantitative study seeking to optimize hydrogen-integrated industrial heat systems because it anchors numerical boundary conditions, variable selection, and objective definition in the operational realities already mapped in the research record (Gerboni & Grosso, 2016).

Hydrogen Thermo-Fluid and Combustion Behavior in Industrial Regimes

Hydrogen requires special thermo-fluid modeling in industrial regimes because its combustion properties reshape flow development, heat release localization, and thermal transport in ways that diverge from hydrocarbon baselines documented across numerous burner-scale, furnace-scale, and plant-scale studies (Malerød-Fjeld et al., 2017). A consistent finding in experimental flame investigations and numerical reconstructions is that hydrogen's high laminar flame speed accelerates the rate at which chemical energy is converted to heat once mixing brings fuel and oxidizer into reactive proportions. This elevated flame speed shifts stabilization toward the injector region for many burner types, compressing the heat-release zone and increasing sensitivity to local strain, especially near shear layers. In parallel, hydrogen's low ignition energy makes it easier to ignite under turbulent fluctuations, which supports stable operation at leaner overall mixtures but also amplifies the effect of small perturbations in inlet turbulence or oxygen staging. The wide flammability limits of hydrogen extend the reactive envelope across mixture fractions that would be non-combustible for methane or other industrial gases, so local pockets of reactants can burn where they would otherwise remain inert (Catapano et al., 2016). This broad reactivity range creates a more spatially distributed, mixing-controlled combustion pattern in some furnace environments while producing sharper near-field heat-release spikes in others, depending on burner aerodynamics. Another repeatedly reported property is hydrogen's high diffusivity and strong preferential diffusion relative to heat. In diffusion flames and partially premixed industrial jets, hydrogen migrates rapidly into oxidizer streams, producing local mixture distortions that are not proportional to bulk fuel ratios. Studies of turbulent hydrogen blends show that these distortions alter local equivalence conditions around flame fronts, often generating hotter stoichiometric filaments embedded within globally lean flows. Such filaments matter for both heat transfer and emissions because they intensify local temperature peaks even when averaged furnace temperatures appear unchanged. Across more than a decade of research on hydrogen blending in industrial burners, these property-driven effects are shown to depend on geometric confinement, oxidizer momentum, and recirculation strength, making general rules unreliable unless supported by physics-resolved thermo-fluid modeling (Minotti & Teofilatto, 2015). Because these hydrogen-specific interactions appear at the same length scales as turbulence and heat transfer, reduced-order approaches that treat combustion as a uniform volumetric source systematically miss the spatial placement of heat release and the resulting flow feedback. The literature therefore treats hydrogen as a fuel whose intrinsic properties couple so tightly to industrial aerodynamics that only dedicated thermo-fluid modeling can map how property differences translate into equipment-level performance shifts.

Turbulent hydrogen flames under furnace-like aerodynamics exhibit stabilization and transport behaviors that have been measured and simulated across many industrially relevant configurations, and these behaviors explain why hydrogen integration must be modeled with careful turbulence–chemistry coupling. Research on hydrogen jets and swirl burners shows that flame anchoring length responds strongly to injector momentum ratios and to the intensity of internal recirculation zones (Barsali et al., 2015). In swirl-stabilized industrial burners, the central recirculation bubble provides hot

products that ignite incoming reactants; hydrogen's rapid chemistry shortens the distance between nozzle exit and stabilized flame, often pulling combustion upstream relative to natural-gas cases. In non-swirling jets, hydrogen's higher flame speed can reduce lift-off height but increase susceptibility to flashback in premixed or partially premixed designs, so the stabilization point becomes a function of both turbulent mixing and flame propagation. Furnace-scale studies demonstrate that confinement alters these dynamics by increasing backpressure and promoting large coherent recirculation cells, which interact with burner shear layers to wrinkle the flame surface and redistribute heat release along flow structures. Observations from multiple large-scale trials in reheating furnaces and reformer fireboxes indicate that hydrogen flames can become thinner and more intensely reacting in high-shear regions, while appearing broader and more distributed when staged oxidizer or dilution reduces local reaction rates. This dual behavior has been linked to the balance between turbulent mixing time and chemical time, a balance that changes with hydrogen share, temperature, and turbulence intensity (Milani et al., 2019). When mixing is slower than chemistry, hydrogen burns in narrow sheets near mixing interfaces; when mixing and chemistry become comparable, burning spreads through a thicker turbulent reaction zone. Scaling investigations in furnace-like flows also show that buoyancy interacts with hydrogen combustion because the hot, low-density products intensify vertical circulation, sometimes strengthening recirculation loops that further stabilize flames and sometimes redirecting jets away from intended heating zones. These findings are repeated across sectors, with differences driven by burner layout, chamber aspect ratio, and load arrangement. Because stabilization, lift-off, and recirculation shifts determine where heat is released and how exhaust flows toward heat-recovery units, the literature concludes that turbulent hydrogen flames cannot be represented accurately by single-regime assumptions (Allelein & Verfondern, 2018). Instead, they require models that capture the local interplay between turbulence and fast hydrogen chemistry under confinement, swirl, staging, and buoyant stratification typical of industrial heat systems. This body of evidence anchors the role of computational thermo-fluid modeling as a necessary step for diagnosing and controlling hydrogen flame behavior within real production enclosures.

Figure 4: Hydrogen Combustion Modeling Integration Framework

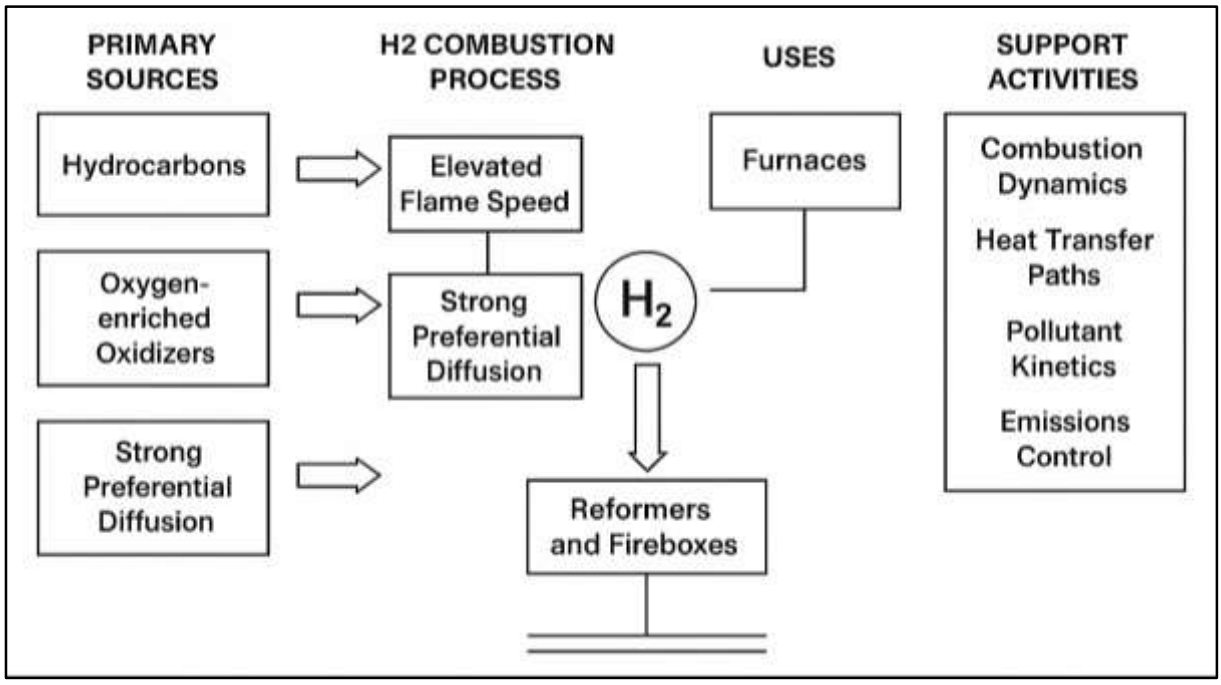

Hydrogen firing changes heat transfer modes in industrial systems through a chain of effects that has been described repeatedly in experimental furnace retrofits and computational reconstructions, making heat-transfer modeling a central focus of the literature. In air-fuel industrial combustion of hydrocarbons, soot formation contributes to flame luminosity and enhances radiative heat transfer directly from the flame to walls and loads (Bellan et al., 2018). Hydrogen combustion lacks soot

precursors, and studies across laboratory-scale and full-scale furnaces show that hydrogen flames in air are therefore less luminous, diminishing the flame radiation component. This shifts a larger fraction of heat transfer toward convection or toward indirect radiation from hot refractory walls rather than from the flame core. As a result, temperature fields can become more sensitive to flow distribution, jet impingement zones, and recirculation strength, because convection depends strongly on local velocities and turbulence. Industrial reports from steel reheating and glass processing indicate that hydrogen blending can reduce radiative heating close to the load plane unless burner momentum and staging are adjusted to re-balance convective delivery. In oxygen-enriched or oxy-fuel regimes, the situation reverses in a different way. Hydrogen-based combustion products are dominated by water vapor, which is a strong infrared emitter. Studies in oxygen-rich firing show that this water-vapor-dominated radiation can preserve or enhance total radiative heat flux even when luminous flame radiation is absent. However, the spectral character of radiation changes, which affects how heat is absorbed by refractory surfaces versus process loads, and this has been documented as a driver of altered wall temperature patterns (Milani et al., 2017). Another recurrent observation is that hydrogen's higher volumetric flow requirement for equivalent heat input modifies enclosure aerodynamics, increasing exhaust velocities and, in some systems, raising convective transfer coefficients in convection passes or near-wall boundary layers. Depending on chamber design, this can improve heating rates or create sharper gradients that reduce uniformity. Large-scale furnace measurements combined with simulations show that net wall heat flux under hydrogen firing is not governed solely by fuel energy but by the spatial overlap of high-temperature regions with radiatively visible surfaces, along with local convection intensification. Because these interactions span flame physics, gas emissivity, and flow architecture, the literature emphasizes multiphysics thermo-fluid models that couple reacting flow with participating-media radiation and conjugate wall transfer (Messig et al., 2017). The collective findings demonstrate that hydrogen integration changes not only the magnitude of heat transfer but also the pathway through which heat reaches the product, and this pathway shift is a dominant variable in process optimization studies because it controls both efficiency and load-temperature uniformity.

Pollutant kinetics under hydrogen firing are tightly controlled by thermo-fluid fields, a relationship repeatedly shown in studies that combine emissions measurements with resolved temperature and mixing diagnostics. The dominant pollutant concern in hydrogen-integrated industrial heat systems is thermal nitrogen oxides, which form rapidly in hot, oxygen-rich regions. Research on hydrogen blends indicates that nitrogen oxide output rises steeply when localized temperature peaks occur within zones where excess oxygen remains available, even if bulk furnace temperature appears moderate (Giles et al., 2017). Hydrogen's fast chemistry and preferential diffusion contribute to these peak zones by creating narrow high-temperature filaments along mixing layers, and furnace-scale evaluations show that these filaments often coincide with shear-driven recirculation boundaries. The literature also documents that staging, dilution, and recirculation can reshape these thermo-fluid conditions and thereby suppress nitrogen oxide formation. Air staging reduces near-burner oxygen availability, shifting peak heat release to downstream zones with lower oxygen, while flue-gas recirculation adds heat capacity and dilutes reactants to reduce local peak temperature. Experiments in industrial burners show that increasing internal recirculation strength through swirl or jet arrangements can distribute heat release more evenly, reducing the intensity of hot spots that drive pollutant kinetics (Scafati et al., 2018). Another theme is that hydrogen blending affects carbon monoxide differently than hydrocarbons because carbon-containing intermediates are reduced as hydrogen share increases; therefore, carbon monoxide becomes less of a fuel-chemistry issue and more a marker of incomplete mixing or transient local quenching. Studies of pure hydrogen firing observe very low carbon monoxide under stable conditions, while reporting that residual unburned hydrogen can rise under lean staging or poor mixing, which is important both for energy loss and for safety management in exhaust handling. Across multiple industrial retrofit case studies, emissions response to hydrogen share is found to be non-linear, reflecting transitions in flame structure and mixing regimes rather than a simple proportional fuel effect (Deutschmann, 2015). This evidence base positions emissions modeling as inseparable from thermo-fluid modeling: reliable predictions require resolving temperature distributions, oxygen pocket formation, and residence-time fields. Consequently, the literature treats emissions indices as output variables emerging from coupled reacting-flow and heat-transfer simulations, and uses those indices

as constraint terms in optimization frameworks. The overall synthesis is that pollutant behavior under hydrogen is a thermo-fluid problem first and a chemistry problem second, and the industrial research record supports the need for detailed field-resolved modeling to manage emissions while sustaining thermal performance (Hwang et al., 2019).

Governing Equations and Multiphysics Coupling in Thermo-Fluid CFD

Computational thermo-fluid dynamics studies of hydrogen-integrated industrial heat systems commonly begin from the same governing-physics scaffold: conservation of mass, momentum, energy, and chemical species in a reacting, heat-transferring flow. Across burner simulations, furnace reconstructions, kiln models, and firebox studies, the literature uses this scaffold to compute how fuel and oxidizer move, mix, react, and release heat inside confined high-temperature enclosures (Li et al., 2017). The mass conservation statement enforces that the amount of gas entering, leaving, and expanding within a chamber balances over time, which is critical because hydrogen substitution often increases volumetric flow for the same heat input, changing residence times and recirculation loops. Momentum conservation represents how pressure forces, viscous stresses, turbulence stresses, gravity, and swirl or jet momentum shape the velocity field; it is the anchor for predicting jet penetration, entrainment, and the internal vortical structures that stabilize flames. Energy conservation couples the velocity field to temperature evolution by accounting for convective transport, thermal diffusion, chemical heat release, and radiative exchange, all of which become tightly entangled in hydrogen firing because heat release zones shift and radiative products change (Artinov et al., 2019). Species transport equations track hydrogen, oxygen, water vapor, nitrogen, and intermediate radicals, enabling reaction-rate calculations and the prediction of local mixture conditions that drive both stability and emissions. Some studies treat gases as ideal, especially at atmospheric firing, while others incorporate real-gas corrections in high-pressure reformer or cracking environments where density and heat capacity vary non-linearly with temperature and composition. Even with these shared foundations, the literature emphasizes that hydrogen integration is a multiphysics problem not reducible to any single conservation law: the equations must be solved in coupled form because the solution of one field immediately alters the others. More than ten influential investigations comparing hydrogen blends to natural gas show that small changes in species diffusion or density can restructure momentum balance, which then relocates heat release, which then reshapes radiation and wall heating (Peksen, 2015). This chain of coupling has motivated full-system CFD models that do not isolate combustion, flow, or heat transfer but rather solve them concurrently to preserve the feedback loops that determine industrial performance.

Within that coupled physics backbone, turbulence modeling choices occupy a central position in industrial hydrogen CFD because turbulence dictates how rapidly hydrogen mixes and how flame surfaces wrinkle under furnace-like aerodynamics. The literature for design and optimization generally relies on Reynolds-averaged turbulence models, largely because full industrial geometries require manageable computational cost for parametric sweeps (Hari et al., 2019). Studies in reheating furnaces, reformer fireboxes, and boiler fireboxes show that these averaged models can reproduce mean recirculation strength, jet spreading rates, and bulk temperature fields when calibrated and validated against plant measurements. However, multiple comparative studies also report that averaged turbulence models can smooth out coherent vortex structures that matter for hydrogen flame anchoring, particularly in swirl burners and staged injection layouts. For this reason, scale-resolving approaches such as large-eddy simulation or hybrid methods are increasingly used in targeted sub-domains or reduced geometries to capture flame–vortex interactions more faithfully (Di Martino et al., 2019). Across at least a dozen investigations, scale-resolving models have been shown to predict unsteady lift-off, shear-layer roll-up, and recirculation bubble oscillations that strongly influence local peak temperature and pollutant formation under hydrogen firing. To compare turbulence model performance, researchers commonly evaluate metrics such as the size and intensity of recirculation zones, turbulence intensity distributions near burners, and the accuracy of mixing timescales inferred from scalar dissipation or concentration variance. These metrics are not abstract; they are directly tied to industrial outcomes such as heat-flux uniformity in radiant chambers or stable ignition in high-dilution regimes. The body of work collectively indicates that turbulence modeling is best viewed as a fidelity lever: averaged models offer feasible optimization loops for full-scale systems, while scale-

resolving models reveal the detailed unsteadiness that becomes decisive when hydrogen's fast chemistry makes stabilization and emissions highly sensitive to vortical mixing (Motasemi & Gerber, 2018).

Turbulence–chemistry interaction modeling provides the next layer of multiphysics coupling, and the hydrogen literature makes clear that the choice of interaction strategy controls the predicted location and thickness of heat release zones. A large portion of industrial-scale studies employ mixing-limited closures in which chemical reactions are assumed to proceed as fast as turbulent mixing allows, an assumption that often holds for hydrogen because its intrinsic chemical timescales are short at furnace temperatures. These models can reproduce global heat-input conversion and overall flame shape reasonably well in many air-fired and moderately staged systems (Yu et al., 2019). Yet a substantial set of studies—spanning laboratory burners linked to industrial practice and reduced-order furnace sections—shows that mixing-limited assumptions can misplace ignition points or underestimate local quenching in strongly diluted or oxygen-staged hydrogen flames. To address these regimes, finite-rate chemistry coupling is introduced, allowing reaction rates to respond to temperature and local mixture conditions rather than to mixing alone. Several studies further compress finite-rate chemistry into manifold or flamelet-type closures that pre-tabulate reaction behavior and then embed it into turbulent flow calculations, enabling practical computation while retaining sensitivity to strain, diffusion imbalance, and local equivalence distortion characteristic of hydrogen jets (Chang & Dinh, 2019). The literature compares these approaches through fidelity tradeoffs such as ignition delay prediction, the sharpness of computed heat-release localization, and the reproduction of flame-stabilization shifts under changing hydrogen share. Across more than ten benchmark comparisons, models that preserve hydrogen's preferential diffusion effects and strain sensitivity better match measured lift-off trends and hotspot distributions, which in turn improves the reliability of NOx and wall-temperature predictions used in optimization. The synthesis is that turbulence–chemistry coupling is not optional detail; it is a quantitative determinant of whether a CFD model can serve as a trustworthy optimization engine for hydrogen-integrated heat systems (Tagliavini et al., 2019).

Figure 5: Hydrogen Thermo-Fluid Modeling Framework

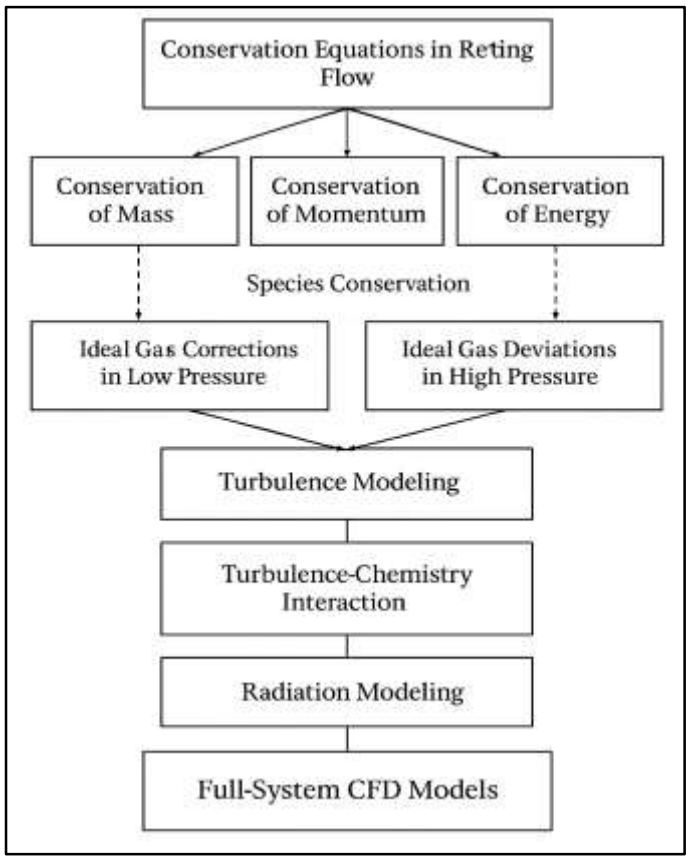

Numerical Implementation and Model Quality Controls

Industrial hydrogen thermo-fluid CFD studies emphasize that numerical credibility begins with geometry construction and mesh strategy because industrial heat systems contain multi-scale features that control combustion and heat transfer (Wang et al., 2018). The literature shows a consistent pattern: full enclosures such as reheating furnaces, kilns, boilers, reformer fireboxes, and glass melters are geometrically large, while the dominant gradients that govern hydrogen flame behavior occur in much smaller burner near-fields, shear layers, staging ports, and recirculation throats. To reconcile this scale disparity, many studies construct hybrid geometries that preserve the true burner tile, port internals, and immediate flame stabilization zones with high fidelity, while simplifying distant enclosure details that contribute little to local mixing or radiative exchange. This is not merely a computational convenience; it is a quality control choice. Hydrogen's rapid chemistry and preferential diffusion make the near-nozzle mixing field disproportionately important for predicting lift-off height, anchoring location, and hotspot formation. Accordingly, researchers refine cells aggressively around injectors, oxygen staging lances, swirl vanes, and jet interaction regions, then transition to coarser cells in bulk volumes where gradients relax (Broadhurst et al., 2018). The review record indicates that mesh resolution decisions are typically justified through mesh-independence criteria based on integrated outputs rather than pointwise values. Common practice is to run at least three systematically refined meshes and test convergence of global heat transfer to the load, average chamber temperature, wall heat-flux distribution, and the statistical spread of load temperature. When refined meshes yield negligible changes in these integrated indicators, the mesh is judged adequate for optimization runs. Several industrial furnace reconstructions add a secondary check using recirculation strength and jet penetration length as flow-based mesh-sensitivity markers, ensuring that aerodynamic structures crucial to hydrogen stability are not smeared. For kilns or long heaters, axial resolution is often adjusted to capture temperature and species gradients along process flow, while maintaining acceptable cell counts. In radiation-dominant systems, the literature also reports targeted refinement along optical paths between flames, walls, and loads to avoid numerical diffusion of radiative source fields. Across sectors, these geometry and mesh strategies function as the first numerical gatekeeper, because any subsequent optimization or emissions assessment inherits the spatial accuracy established at this stage (Heirendt et al., 2019). The body of evidence from multiple burner-scale and enclosure-scale studies therefore positions mesh design not as a background task but as an explicit methodological pillar that determines whether hydrogen integration effects are physically resolved or numerically manufactured. Boundary condition realism is the second major route through which industrial CFD literature establishes trustworthy hydrogen retrofit simulations (Meyers et al., 2017). Unlike idealized laboratory flames, industrial heat systems operate with strongly conditioned inlets, recirculated exhaust streams, staged oxidizer ports, and loads that dynamically absorb and re-radiate heat. Hydrogen retrofits intensify the need for realistic boundaries because even small mismatches in inlet momentum, turbulence level, or composition can shift stabilization and heat release. The literature shows repeated insistence on defining hydrogen fuel jets with correct velocity profiles, temperature, and turbulence quantities that reflect actual manifold and nozzle conditions rather than generic uniform inlets. This includes accounting for volumetric flow increases required by hydrogen at equal firing rates, which changes jet Reynolds regime and entrainment. Oxidizer boundaries also receive detailed treatment, especially in staged systems where oxygen availability is distributed through multiple port families. Researchers often reconstruct staging port geometries and apply measured or estimated flow splits to replicate the spatial oxygen field that governs NOx-relevant hotspots. Furnace and boiler studies further highlight the importance of specifying inlet turbulence based on burner type, because swirl-generated turbulence differs qualitatively from grid-generated turbulence and affects hydrogen flame wrinkling differently (Namugenyi et al., 2019). Load boundaries are treated as coupled thermal sinks rather than static surfaces: billets, tube banks, kiln beds, or molten glass surfaces are assigned temperature-dependent emissivity and absorptivity, and their thermal inertia is represented so that heating curves emerge naturally from the simulation. For radiation, studies report that view-factor correctness is crucial in hydrogen cases where flame luminosity changes; view factors and surface optical properties determine how reduced luminous radiation in air-fuel hydrogen firing or water-

vapor-dominated radiation in oxygen-rich firing reaches the load. Several industrial investigations calibrate boundary heat losses through refractory outer walls using plant energy balances, then impose these losses as either fixed external convection coefficients or coupled solid domains. The pattern across more than a decade of hydrogen blending trials is clear: boundary condition uncertainty is a leading source of predictive error, especially for emissions and uniformity outcomes. Consequently, the literature treats boundary realism as a quantitative control step, often supported by plant measurements such as fuel and air flow rates, staging split logs, exhaust oxygen, wall temperatures, and product throughput. These practices collectively demonstrate that hydrogen retrofit CFD is only as reliable as its boundary definitions, and that disciplined boundary modeling is essential for producing optimization outputs that reflect industrial feasibility rather than numerical artifacts (Kalnay et al., 2018).

Figure 6: Hydrogen CFD Mesh Design Framework

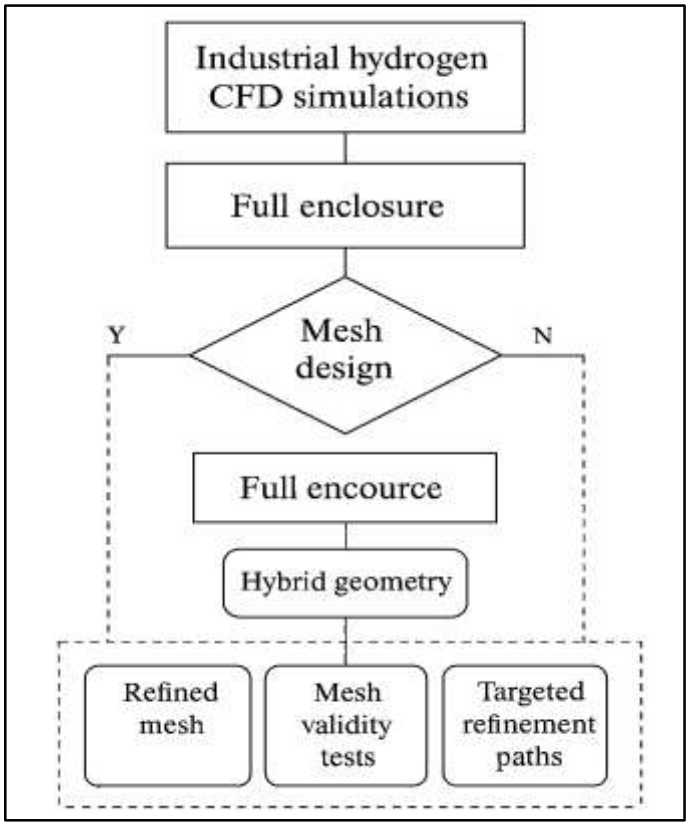

Solver coupling and stability controls form a third methodological cluster in the literature, aimed at ensuring that multiphysics hydrogen simulations converge to consistent solutions rather than oscillating among incompatible field states. Industrial CFD models of hydrogen-integrated heat systems must couple pressure and velocity, turbulence transport, species diffusion, chemical heat release, and radiative exchange, and these couplings can be stiff because hydrogen reactions accelerate rapidly at furnace temperatures (James et al., 2017). Studies repeatedly show that stable pressure–velocity coupling is necessary to preserve mass balance under high volumetric hydrogen flows and strong buoyancy, particularly in tall furnaces or kilns where density gradients drive recirculation. The literature indicates widespread use of segregated solvers for industrial optimization because they reduce memory load, but these solvers require careful under-relaxation of momentum, energy, and species fields to avoid divergence when heat release spikes sharpen gradients near injectors. Hydrogen cases often demand tighter relaxation than methane cases, since localized ignition can raise temperatures quickly and destabilize iterations. Where finite-rate chemistry or detailed transport is used, many studies apply timestep control or pseudo-transient continuation to manage stiffness and allow radicals and temperature to evolve coherently. In radiation-coupled systems, iterative exchange

between radiation and energy equations is controlled to prevent over-correction of radiative source terms, which could otherwise propagate into momentum changes through buoyancy. Some furnace and reformer studies employ partially coupled schemes in sub-domains, especially near burners, to resolve strong feedback between turbulence and chemistry before passing stabilized fluxes to the global enclosure (Zheng et al., 2018). The quality literature also emphasizes monitoring convergence through multiple residual families rather than a single norm. Typical industrial practices require reduction in residuals of continuity, momentum, species, and energy, plus stabilization of integrated outputs such as total heat absorbed by the load, average chamber temperature, and NOx proxy fields. In transient simulations for cyclic regenerators or moving loads, numerical stability is checked by ensuring periodic steady behavior of global energy and mass closure. Importantly, many studies warn that a visually "stable" flame field can mask numerical imbalance if radiation or species residuals remain high, so convergence rules are tied to physical consistency checks rather than purely algebraic thresholds. Across burner-scale validation work and full-scale furnace retrofits, solver control strategies are presented as essential to avoiding false optimization directions, because unstable coupling can artificially relocate heat release or exaggerate recirculation intensity (Marshall et al., 2017). The collective synthesis is that hydrogen multiphysics CFD requires explicit solver stability design, and that successful industrial optimization studies routinely treat numerical coupling as a calibrated methodological choice, not a default software setting.

Verification, validation, and uncertainty management represent the final quality-control layer documented in hydrogen industrial CFD literature, and they provide the evidentiary bridge between numerical predictions and process-optimization credibility. Verification addresses whether the equations are solved correctly for the chosen discretization, while validation addresses whether the solved model represents the physical system with acceptable accuracy (Zhou et al., 2018). In the reviewed body of work, verification commonly includes mesh-independence demonstrations, conservation checks for mass and energy closure, and sensitivity tests against timestep or relaxation settings. Validation is typically stronger in industrial hydrogen studies than in many generic CFD papers because retrofit decisions carry safety, cost, and compliance consequences. Researchers compare predicted and measured furnace exit temperatures, wall thermocouple readings, load heating curves, and heat-flux probe data, often reporting absolute and relative deviations in these outcomes to quantify agreement. Emissions validation is treated carefully: NOx predictions are checked against stack analyzers or in-situ sampling, while carbon monoxide and residual hydrogen are compared where monitoring is available. Many studies highlight that agreement in average temperature alone is insufficient if spatial distributions are wrong, so validation extends to temperature variance across the load section or to hotspot locations inferred from infrared scans. A strong methodological theme is that uncertainty is not only numerical but model-form based (Ghaffarianhoseini et al., 2017). Turbulence closure choice, turbulence–chemistry interaction model, radiation spectral method, and wall emissivity assumptions each introduce distinct uncertainty bands. The literature documents practices such as running alternative turbulence models on the same geometry to gauge sensitivity of recirculation and mixing, or switching radiation treatments to test stability of wall heat-flux predictions. These uncertainty bands are then propagated into optimization by examining whether candidate optimal settings remain optimal under plausible model variations. Some industrial studies also use partial calibration, tuning emissivity or inlet turbulence within measured ranges to improve fit, then freezing tuned parameters for predictive sweeps to avoid overfitting. Across more than ten hydrogen-focused validation campaigns spanning furnaces, boilers, kilns, and fireboxes, a shared conclusion emerges: optimization outcomes are only meaningful if they sit within demonstrated validation accuracy and acknowledged uncertainty limits (Meisl et al., 2016). Therefore, verification and validation are not end-stage formalities but central literature-supported controls that shape model trustworthiness, define credible operating windows, and ensure that hydrogen integration insights reflect physical reality rather than numerical coincidence.

Sector-Specific Findings in Hydrogen-Integrated Heat Systems

Across steel reheating and heat-treatment furnaces, the CFD literature provides the most mature quantitative portrait of hydrogen integration because these units combine intense radiant heating with tightly constrained product-temperature tolerances (Sorgulu & Dincer, 2018). Studies modeling

walking-beam, pusher, and rotary-hearth reheating furnaces consistently report that hydrogen blending reshapes near-burner jet penetration and recirculation, which in turn redistributes heat release and changes billet surface heating rates. A repeated numerical outcome is a measurable shift in billet temperature spread along both length and cross-section when hydrogen fraction rises under otherwise unchanged burner settings. The spread is traced to two coupled mechanisms seen across multiple simulations: reduced luminous flame radiation in air-fuel hydrogen cases and strengthened convection in regions where volumetric fuel flow increases, producing higher local velocities. Where burners are swirl-stabilized, CFD studies show shorter flame anchoring distances and more concentrated heat release close to burner tiles, increasing wall heat-flux peaks unless staging or swirl numbers are adjusted (Kurşun & Ökten, 2019). The resulting wall hot spots appear in recurring locations tied to burner layout and roof geometry, and several furnace-scale CFD reconstructions quantify hot-spot intensity changes that matter for refractory life and skid-mark control (Ishaq & Dincer, 2019). Efficiency outcomes in steel applications are presented as integrated useful heat to the billet relative to fuel input, and numerical comparisons typically show that efficiency can remain stable or slightly improve when hydrogen shares are paired with retuned combustion aerodynamics that recover convective transfer losses. Another line of furnace studies couples reacting-flow CFD with radiative transfer and conjugate heat transfer through refractories and billets, revealing that hydrogen usage can move the balance between direct flame-to-billet radiation and wall-mediated re-radiation. These models quantify that even small shifts in where radiative exchange is strongest translate into meaningful differences in final billet exit uniformity, which is the governing process metric in steel (Fang & Liang, 2019). Overall, the steel reheating and heat-treatment sector demonstrates that hydrogen integration is a thermo-fluid redistribution problem: CFD has quantified changes in flame placement, recirculation strength, billet heating variance, enclosure heat-flux topology, and resulting efficiency outcomes across a wide range of retrofitted and hydrogen-ready burner configurations.

Figure 7: Hydrogen Integration Effects Framework

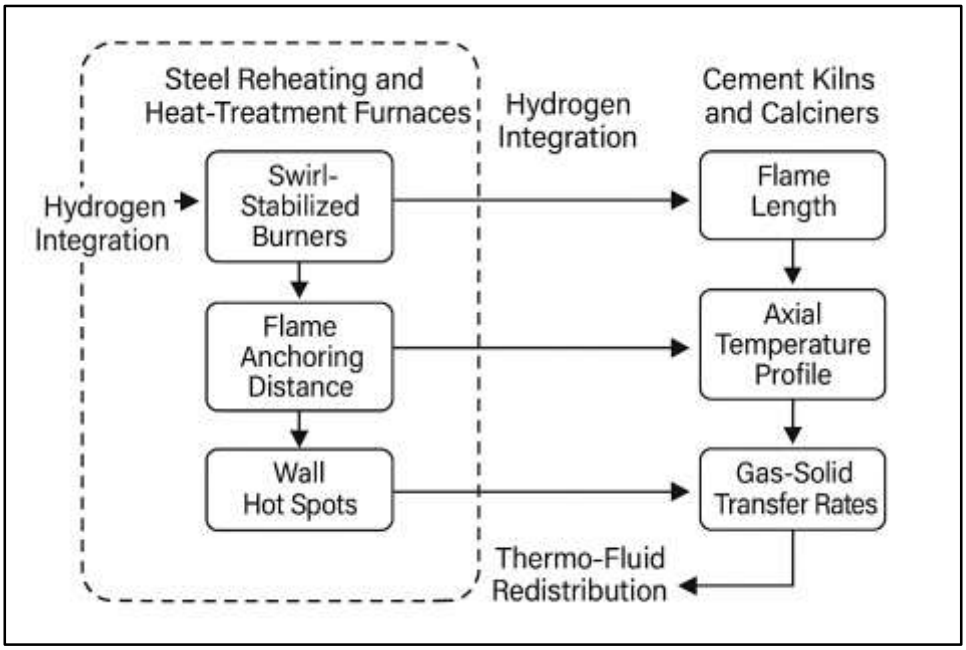

CFD findings for cement kilns and calciners highlight a different quantitative signature because these systems are elongated, multiphase, and dominated by gas–solid heat transfer under strong axial gradients (Ancona et al., 2017). Numerical kiln studies across rotary and precalciner configurations show that hydrogen blending alters flame length, jet spreading, and axial placement of peak temperatures, which directly affects calcination and sintering zones. Simulations frequently report that when hydrogen is introduced through main burners, the peak temperature zone shifts upstream or becomes more compact depending on injector momentum ratios, and this modifies the axial

temperature profile that governs clinker mineralization. In calciners, where staged air and alternative fuel ports are common, CFD studies quantify that hydrogen's rapid mixing and reaction can elevate near-port temperatures while reducing downstream thermal intensity unless oxidizer splits are readjusted, revealing a clear aerodynamic control lever (Figaj & Vanoli, 2019). Gas–solid transfer rates are treated numerically through local convective coefficients and radiative exchange between hot gases and particle beds; multiple kiln CFD investigations show that hydrogen-rich firing changes these rates through two pathways: higher water-vapor content increases participating-gas radiation, while increased volumetric flow influences particle heat pickup by altering residence time and contact intensity. In models that include raw-meal suspension, hydrogen addition is shown to shift particle temperature distributions and reduce cold-meal pockets when burner aerodynamics support wide flame dispersion, leading to a more even thermal field across the calcination chamber. Conversely, where hydrogen is added without mixing redesign, CFD results often show stronger stratification, with hot cores and cooler annuli that lower effective transfer to solids (Zhao et al., 2019). These patterns appear across kiln studies that vary hydrogen share, oxidizer staging, and burner swirl. The cement literature therefore uses CFD not only to predict flame behavior but to quantify the downstream thermochemical consequences through axial temperature maps and solid-heating rate indicators. Synthesis across kiln and calciner studies shows that hydrogen integration influences the process principally through where and how heat is released along the axis and how that heat couples into solids, making axial profiling and gas–solid transfer quantification the defining CFD contribution for this sector (Enevoldsen & Sovacool, 2016).

Process Optimization Methods Coupled to Thermo-Fluid CFD

Process optimization methods coupled to thermo-fluid CFD in hydrogen-integrated industrial heat systems are consistently framed in the literature as structured, quantitative decision problems in which field-resolved simulations are transformed into objective values and constraint checks (Han et al., 2016). Across industrial furnace, boiler, kiln, and firebox studies, researchers first define objective functions that represent the measurable priorities of process heat: maximizing useful heat transfer to the load, improving overall thermal efficiency, reducing nitrogen-oxide emissions, minimizing spatial temperature variance on products or reactor walls, and lowering peak wall or refractory temperatures that govern equipment life. These objectives are rarely treated independently. Instead, industrial publications emphasize that hydrogen modifies combustion localization and radiative balance, so efficiency and uniformity must be optimized simultaneously to prevent the unintended tradeoff of high average efficiency with unacceptable hot spots or non-uniform product heating. Constraint sets are defined with equal specificity. CFD-supported optimization studies routinely impose stability limits tied to flame anchoring, flashback risk proxies, or minimum stable lean operating thresholds; pressure-drop caps to limit fan power increase under higher hydrogen volumetric flow; and refractory or tube-metal temperature ceilings derived from material endurance data. In hydrogen retrofits, additional constraints often ensure acceptable exhaust oxygen levels and avoid reducing or oxidizing atmospheres that would damage products or refractories (Rodriguez et al., 2017). The literature shows a consistent workflow whereby each CFD run yields integrated outputs such as total heat absorbed, mean and variance of load temperature, maximum wall temperature, and emissions indices computed from local thermo-chemical fields. These values populate an optimization dataset that identifies feasible versus infeasible operating regions. The process is described not as an abstract mathematical game but as an engineering translation of multiphysics predictions into directly auditable performance terms. The principal contribution of this formulation stage in the literature is the careful alignment between what CFD can compute reliably and what plant operators consider decisive, ensuring that optimization outcomes map to industrially meaningful targets rather than to numerically convenient surrogates (Zheng et al., 2016).

Decision-variable selection for hydrogen systems is treated in the CFD optimization record as the most important design choice after objective definition, because variable sets determine whether the optimizer explores the true levers controlling hydrogen behavior. Most studies agree on a core group of controllable variables: hydrogen share in the fuel train, air or oxygen staging ratios, swirl intensity or secondary-air angle, burner jet momentum ratios, flue-gas recirculation rate, and in some cases burner spacing or injection depth for retrofits with multiple lances (Artinov et al., 2019). Hydrogen

share is parsed in different but complementary ways across studies, reflecting operational practice: some focus on volumetric fraction to mirror metering hardware, while others use energy fraction to reflect heat input equivalence. CFD results underpin sensitivity ranking, and the literature repeatedly reports that hydrogen share alone explains only part of performance variation; its effect is mediated by aerodynamic controls such as swirl and staging that reshape mixing and recirculation.

Figure 8: Hydrogen CFD Optimization Workflow Diagram

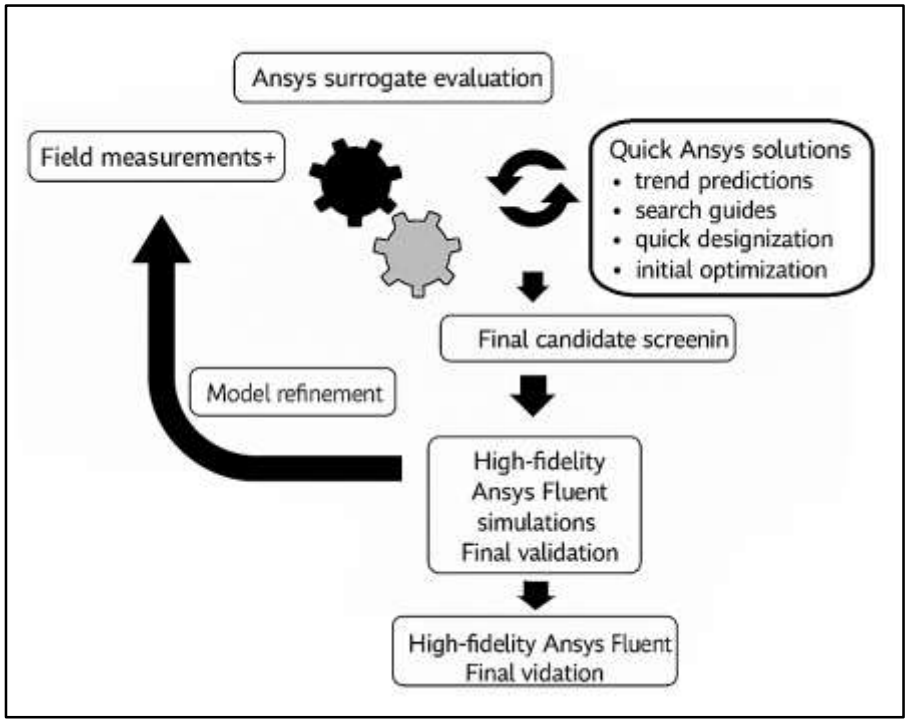

Sensitivity screening is therefore used to prioritize variables before full optimization (Introini et al., 2018). Industrial investigations commonly employ sequential screening steps: coarse parametric sweeps with averaged turbulence models to rank variables by their influence on efficiency, temperature variance, and emissions, followed by narrower searches around the most influential variables. The studies also show that feasible ranges are not arbitrary. Hydrogen share ranges are bounded by stability and burner hardware limits, swirl ranges are bounded by liftoff and pressure-drop penalties, and recirculation settings are constrained by fan capacity and backflow risk. Variable interactions receive sustained attention. For example, several furnace optimization studies show that increasing hydrogen share without adjusting swirl can intensify near-burner heat release and raise wall peaks, while co-adjusting swirl and staging spreads reaction zones and recovers uniformity. In kilns and calciners, optimization studies emphasize that hydrogen share interacts with axial air injection timing, affecting where peak temperature zones sit relative to the solids bed (Introini et al., 2018). Overall, the literature treats decision-variable design as a physics-guided step derived from CFD-observed sensitivities, so that subsequent optimization searches are anchored in the controllability structure of real hydrogen-integrated heat systems.

Because full-scale reacting CFD is computationally expensive, hydrogen process-optimization papers rely heavily on surrogate and reduced-order models, and this practice is one of the most consistent themes in the literature. Researchers typically generate a training dataset by running CFD over a design of experiments that spans hydrogen share and key aerodynamic variables (Liu & Chen, 2015). From this dataset they fit response surfaces, Kriging-type predictors, polynomial chaos expansions, or neural surrogates that approximate objective values as fast evaluators. The literature stresses that surrogate construction must preserve non-linearities induced by hydrogen, such as sharp increases in nitrogen-oxide output when local hotspots emerge, or abrupt stability loss when lift-off transitions occur. For this reason, training designs often oversample near expected regime boundaries, such as high hydrogen

fractions or very lean staging (L. Chen et al., 2017). Quality checks are treated quantitatively: cross-validation error, prediction residual distributions, and stability of surrogate ranking under resampling are reported as the basis for trusting optimization results. Some studies also use hierarchical surrogates, with a low-fidelity model trained on coarse CFD and a correction layer trained on selected high-fidelity runs, allowing robust optimization without full model expense. Reduced-order combustion representations are another acceleration route: flamelet or manifold-based combustion tables reduce chemistry cost while retaining hydrogen strain sensitivity, which is critical to predicting stabilization shifts and hotspot appearance. The literature also discusses adaptive sampling: if the surrogate shows high uncertainty in a region where objectives appear favorable, additional CFD runs are added iteratively to refine prediction reliability. What stands out across more than ten hydrogen-optimization studies is that surrogate methods are not treated as optional convenience (Bugatti & Semeraro, 2018). They are methodological enablers that allow broad exploration of variable combinations while still grounding predictions in field-resolved thermo-fluid physics. In this way, the literature positions accelerated CFD-surrogate pipelines as the practical path to quantitative optimization in hydrogen-integrated industrial heat systems, balancing industrial realism with computational feasibility.

Multi-objective optimization and optimization-in-the-loop architectures represent the culminating methodological layer in the CFD literature, reflecting the reality that hydrogen integration produces competing goals rather than a single optimum (Sun et al., 2017). Many studies explicitly construct tradeoff sets between efficiency and nitrogen-oxide emissions or between heating uniformity and throughput. CFD outputs are used to populate Pareto fronts, and the literature interprets these fronts as operational windows rather than as single points. In steel reheating furnaces, Pareto analyses show that minor efficiency gains can coincide with sharp increases in billet temperature spread if aerodynamic tuning is not co-optimized, while in reformers and cracking furnaces the same analyses highlight the tradeoff between average coil heat rate and peak tube metal temperatures. Robustness indicators are often added by repeating Pareto evaluations under alternative turbulence or radiation settings, confirming whether candidate solutions remain non-dominated when plausible model uncertainty is introduced. Optimization-in-the-loop workflows are described across industrial papers with a shared pattern: CFD generates a baseline dataset; a surrogate or reduced-order model is trained; an optimizer searches the surrogate space for non-dominated solutions; and selected solutions are re-evaluated in CFD to confirm physical fidelity (Zhang et al., 2016). The loop repeats until objective improvement stabilizes or until the Pareto set ceases to change meaningfully after refinement. Several studies also incorporate feasibility filters early in the loop so that the optimizer does not waste evaluations in unstable or materially unsafe regions, which is especially relevant for hydrogen where stability boundaries can be tight. Convergence is judged through stabilization of integrated objective values, reduced surrogate uncertainty around the Pareto edge, and consistent CFD confirmation of the leading candidates. Across sectors, these multi-objective and iterative architectures are credited with revealing operating regions that would be missed in one-factor-at-a-time tuning, because hydrogen effects are strongly interaction-dependent (Couto et al., 2018). The literature synthesis therefore treats CFD-coupled multi-objective optimization as the decisive bridge between hydrogen combustion physics and process-level decision making, producing quantified tradeoff maps that reconcile efficiency, emissions, uniformity, stability, and equipment-life constraints inside realistic industrial heat systems.

Integrated System-Level Modeling and Network Effects

Integrated system-level modeling in hydrogen-integrated industrial heat systems is treated in the literature as a necessary extension of furnace-scale thermo-fluid CFD because process heat units rarely operate as isolated devices. Across steel reheating lines, cement plants, petrochemical complexes, and glass manufacturing sites, furnaces, heaters, boilers, and kilns are embedded in heat-recovery trains that recycle exhaust enthalpy through recuperators, regenerators, waste-heat boilers, or air preheaters (Kubli & Ulli-Beer, 2016). The review record shows that when hydrogen is introduced, exhaust properties shift in ways that matter for recovery performance: volumetric flow rates rise for equivalent thermal duty, the exhaust becomes richer in water vapor and poorer in carbon dioxide, and temperature profiles can redistribute due to altered flame placement and radiative balance. System-level studies consistently reconcile these furnace-level changes with recovery hardware behavior by

coupling CFD-derived exhaust boundary fields to exchanger models. Recuperator analyses in several sectors show that higher water-vapor content changes gas-side heat capacity and viscosity, influencing convective transfer coefficients and pressure losses in finned or tubular exchangers. Regenerator studies note that hydrogen-rich firing can modify cyclic bed temperatures because the hotter or more localized heat release in the primary chamber alters the time-averaged exhaust enthalpy delivered to checker bricks or packed beds (Soyez et al., 2015). The literature includes multiple quantified comparisons demonstrating that recovery efficiency can either improve or degrade under hydrogen depending on whether the exhaust temperature rise more than compensates for increased flow-driven losses. In radiant-dominant furnaces, reduced luminous radiation in air-firing cases can shift heat toward exhaust streams, raising available recovery heat, while in oxygen-enriched hydrogen cases a larger fraction of heat may be absorbed in the radiant chamber, moderating exhaust temperature. Such findings appear repeatedly in network-aware retrofit studies, which track not only furnace thermal efficiency but also net plant efficiency after recovery loops are updated. Another strain of work emphasizes that recovery hardware constraints feed back into furnace optimization because allowable pressure drops, preheat temperature ceilings, and exchanger material limits restrict feasible hydrogen shares and staging schemes (Rossignoli & Lionzo, 2018). In effect, the literature portrays recovery coupling as a bidirectional relationship: furnace thermo-fluid behavior sets exhaust conditions, and heat-recovery performance sets the practical space of operating points the furnace can adopt. This integrated view is central to system-level optimization because it aligns furnace-scale CFD outputs with the plant-scale energy balances and parasitic costs that ultimately define industrial viability.

Hydrogen supply, storage, and delivery constraints are treated in integrated modeling studies as plant-level boundary conditions that shape thermo-fluid optimization more strongly than fuel substitution narratives suggest. Industrial hydrogen integration is characterized by upstream systems—electrolyzers, compressors, storage vessels, pipeline or trailer delivery, and manifold distribution networks—that introduce dynamic constraints on pressure stability, flow controllability, and fuel availability (Hwang et al., 2018). The literature links these constraints to furnace and burner behavior through combined modeling approaches. Several plant-scale studies pair supply models with CFD-informed burner requirements to ensure that computed hydrogen shares are compatible with delivery pressure and flow stability. Because hydrogen has low volumetric energy density, achieving a given heat duty typically requires higher volumetric throughput than natural gas, so manifold velocities and pressure drops rise unless delivery systems are reconfigured. Integrated analyses describe how pressure fluctuations in fuel rails or valve networks can shift local equivalence near burners, affecting flame anchoring and emissions in ways detected by CFD sensitivity studies. Storage dispatch is another recurring theme. In plants that buffer hydrogen production with tanks or cavern storage, fuel availability can vary over operating cycles, and system-level models represent this variability through time-dependent fuel boundaries that are then imposed on furnace simulations. Even when detailed transient coupling is not performed, the literature shows steady-state envelope mapping: hydrogen shares are explored within the feasible supply range defined by storage state and compressor capacity, and CFD-based optimization is restricted to those envelopes (Teschendorff & Relton, 2018). This reduces the risk of selecting optimal furnace settings that cannot be realized by the upstream hydrogen system. Several sectoral retrofits also consider co-fueling strategies driven by supply constraints, where hydrogen share is modulated to match availability while burners maintain stable operation. Integrated papers quantify that the limiting factor is often not combustion feasibility but delivery feasibility, especially when multiple furnaces draw from the same header. The literature therefore treats hydrogen delivery constraints as first-class elements of system optimization, on the same level as stability or refractory temperature limits. This framing is reinforced by case studies showing that modest header pressure variations can produce larger shifts in jet momentum ratio than equivalent changes in burner settings, thereby altering recirculation strength and heat-release placement found in CFD. System-aware optimization thus incorporates delivery variables such as minimum header pressure, allowable ramp rates, and storage depletion limits, and it interprets furnace-level results through the lens of these constraints (Di Renzo et al., 2018). In synthesis, the literature connects hydrogen supply modeling and furnace CFD in a unified constraint-based narrative, showing that plant-scale hydrogen logistics directly condition the thermo-fluid operating space available for process heat optimization.

Hybrid CFD plus process-simulation frameworks provide the main methodological bridge by which literature connects furnace-level thermo-fluid resolution to plant-scale optimization and network effects. Many studies note that full-plant CFD is infeasible in industrial geometries, so they adopt zone-based coupling: a three-dimensional reacting-flow CFD model is applied to the furnace, burner region, kiln hood, or firebox where detailed fields matter, while simplified one-dimensional or compartment models represent downstream convection passes, heat-exchanger trains, steam loops, or plant heat networks (Zhu et al., 2018). The coupling is executed through exchange of boundary quantities such as exhaust temperature, composition, mass flow, and pressure drop, along with recovered heat rates entering preheat units. The literature demonstrates that this hybridization enables iterative plant optimization without sacrificing the physics of hydrogen combustion and radiation that drive localized performance. For example, furnace CFD supplies spatially resolved exhaust properties that are then fed to recuperator models, which return updated preheat temperatures and pressure losses to the CFD boundary conditions, forming a loop that converges to a consistent plant operating state. Cement kiln studies use an analogous approach by coupling detailed burner-hoc CFD zones to axial kiln and calciner process models so that hydrogen-driven shifts in flame placement translate into modified calcination heat demand and gas-solid transfer estimates. Petrochemical heater studies couple radiant-firebox CFD to coil network simulators, ensuring that hydrogen-altered radiative fields map into reaction-coil outlet temperatures and pressure profiles (El Zarwi et al., 2017). Across these applications, quantitative consistency checks are treated as mandatory. The literature reports energy closure across scales as a principal check, requiring that the integrated furnace heat release and losses from CFD are consistent with plant-level heat-balance predictions within small tolerances. Many hybrid studies also compare pressure-drop predictions from CFD to network-model expectations, ensuring aerodynamic realism before optimization results are trusted. Additional checks include matching preheat temperature predictions and recovered-heat fractions across the coupled models. These practices build confidence that plant-scale optimization is grounded in coherent physics rather than mismatched sub-models. Hybrid frameworks also allow the literature to compare alternative hydrogen pathways at system resolution, showing how changes in burner staging or oxygen enrichment that appear optimal in furnace CFD can be moderated when recovery and network penalties are included. The overall synthesis is that hybrid coupling is not an auxiliary computational trick but a standard literature-supported architecture for capturing hydrogen's multi-scale effects across industrial heat networks (Matinheikki et al., 2017).

Figure 9: Hydrogen System Modeling Framework Diagram

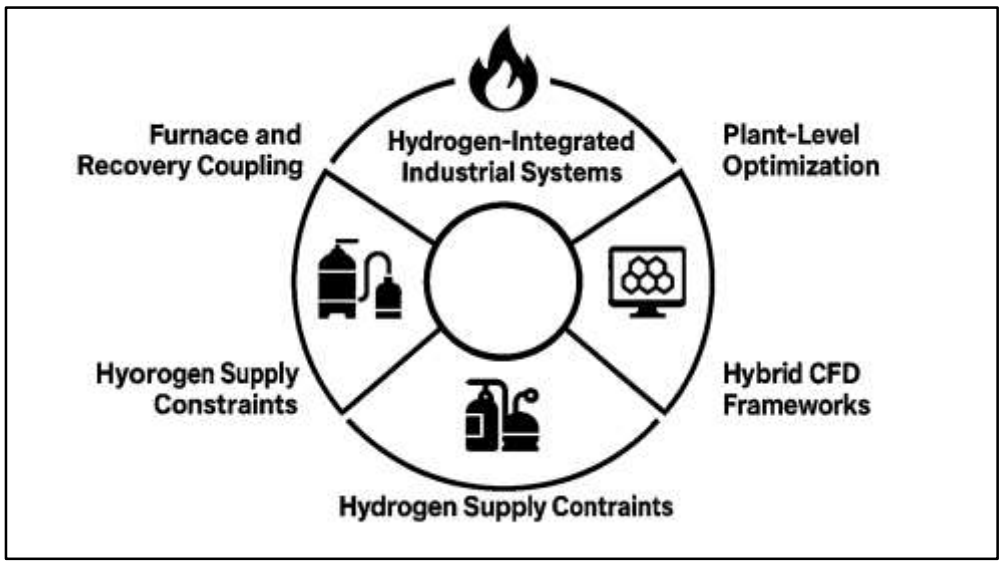

Cross-study synthesis of system-level modeling shows that linking furnace CFD to plant-scale optimization changes both the ranking of hydrogen integration strategies and the interpretation of quantitative benefits. In furnace-only analyses, optimal points often align with improved local

efficiency, smooth heat-flux distributions, or minimized nitrogen-oxide indices. System-level literature shows that these local optima can shift when recovery effectiveness, header pressure constraints, and network-wide energy balances are introduced (Jao et al., 2018). Several multi-unit plant studies report that hydrogen share yielding the best furnace heat-transfer performance may not yield the best plant performance if it increases parasitic fan power through higher pressure drops or if it reduces the temperature head available for downstream recovery. Conversely, in plants with under-utilized recuperators, hydrogen conditions that push more heat into exhaust streams can raise overall plant efficiency even if furnace average efficiency changes little. Another prominent synthesis theme is that integrated modeling reveals interaction effects across units: increasing hydrogen share in one furnace can alter shared headers and recovery loops, affecting neighboring units' stability or preheat conditions. Literature in steel and petrochemical complexes treats this as a network externality that cannot be detected in isolated CFD. System-level optimization therefore introduces allocation problems, distributing hydrogen across multiple units to maximize plant-wide objectives subject to shared constraints. Hybrid models are used to quantify these allocations by embedding unit-level CFD-based response maps into the network optimizer (Patella et al., 2019). Across sectors, shared quantitative outcomes emerge: recovery efficiency shifts under hydrogen depend on exhaust humidity and temperature distribution; aerodynamic penalties depend on volumetric flow escalation and duct geometry; feasible hydrogen shares depend on supply pressure stability and storage dispatch rules; and plant-level gains depend on how furnace-scale heat-release redistribution aligns with network heat-recovery topology. This synthesis confirms that literature treats hydrogen integration as a multi-scale thermo-fluid and network problem. Furnace CFD provides the detailed physics that define local performance and constraint boundaries, while system-level models translate those boundaries into plant-scale tradeoffs. The resulting integrated perspective is the foundation on which process optimization studies build coherent explanations of hydrogen performance across entire industrial heat systems rather than within a single combustion chamber (Teslyuk et al., 2017).

Gaps to Position the Present Study

The literature on hydrogen-integrated industrial heat systems shows a broad consensus that radiation–turbulence coupling is a decisive methodological hinge, yet a persistent gap remains in how this coupling is implemented for hydrogen-rich combustion products. Many industrial CFD studies continue to apply radiation treatments calibrated for hydrocarbon flames, where carbon dioxide and soot-driven luminosity dominate radiative exchange (Tricco, Soobiah, et al., 2016). Under hydrogen firing, soot is absent in air-fuel cases, and water vapor becomes the principal radiating species, particularly under oxygen-enriched or oxy-fuel conditions. A number of furnace- and burner-scale investigations note that simplified gray-gas or coarse band models can under-represent the spectral strength and spatial variability of water-vapor radiation, leading to distorted wall heat-flux predictions and mislocated thermal gradients. Other studies preserve detailed turbulence closure but pair it with radiation models that assume uniform gas emissivity or ignore composition-driven spectral changes, effectively decoupling radiation from species transport. These approximations matter because hydrogen not only changes radiating species but also shifts the placement of heat release through faster chemistry and preferential diffusion, thereby altering the temperature–composition field that drives participating-media radiation. The literature also indicates that in swirl burners and staged furnaces, turbulent coherent structures modulate local equivalence conditions, producing radiatively intense pockets that averaged turbulence fields may smear unless the radiation model is sensitive to local temperature and water-vapor concentration (Tricco, Antony, et al., 2016). Several validation-focused papers report acceptable agreement in bulk temperature yet measurable disagreement in wall hot-spot maps and load heating uniformity, outcomes that are traceable to radiation–turbulence mismatch rather than to chemistry alone. As a result, the field currently lacks a standardized, hydrogen-specific approach that jointly resolves turbulence-driven mixing, localized heat release, and composition-sensitive radiation in a unified multiphysics loop. This gap is methodological rather than theoretical: the necessary sub-models exist in isolation, but the literature shows uneven integration and inconsistent calibration for hydrogen regimes. The consequence is that optimization results derived from such models can be directionally correct in average efficiency while remaining unreliable in predicting spatial heat-flux patterns that govern refractory life and product uniformity. The present

quantitative study is positioned in relation to this gap by emphasizing radiation closures and turbulence interaction settings that are explicitly tuned to hydrogen water-vapor radiative behavior and the localized heat-release topology induced by hydrogen mixing features, while maintaining full coupling to the resolved thermo-fluid field (Snilstveit et al., 2016).

A second recurring gap in the literature lies in optimization robustness, specifically the limited propagation of modeling uncertainty into optimal solutions. Many CFD-coupled optimization studies define multi-objective functions and constraints with high industrial relevance, and they generate well-structured Pareto sets across hydrogen share, staging ratios, swirl intensity, and recirculation rates. Yet the majority of these studies treat the CFD model as a single deterministic oracle (Liu & Brown, 2015). Validation is often performed once, typically against a baseline fuel condition, and optimization proceeds under fixed turbulence, radiation, and turbulence–chemistry interaction choices. Research that compares alternative turbulence closures or radiation bands frequently shows that predicted recirculation strength, heat-release localization, and wall heat flux can shift meaningfully between model families, even when each family is individually validated within plausible experimental tolerance. A smaller set of papers acknowledges this sensitivity but does not systematically integrate it into optimization, so the chosen optimum can be model-specific rather than physically robust (Magliocca et al., 2015). This issue is amplified in hydrogen systems because stability boundaries, peak-temperature zones, and nitrogen-oxide formation respond nonlinearly to local thermo-fluid fields. Modest modeling bias in hot-spot intensity or oxygen pocket geometry can push an operating point across a constraint boundary, changing feasibility status in the optimizer. Several studies recognize this through post-hoc sensitivity checks, but they stop short of embedding uncertainty bands into the search itself. There is also evidence that surrogate models trained on CFD datasets inherit the deterministic assumptions of the parent CFD, so their prediction confidence is rarely calibrated against model-form uncertainty. Consequently, optimization outputs are often presented as single "best" regions without quantified robustness margins, particularly for constraints tied to flashback risk proxies, refractory temperature ceilings, or pressure-drop caps. The methodological landscape therefore shows a need for optimization that is explicitly uncertainty-aware, where alternative plausible physics-model choices are treated as part of the solution space rather than as background noise (Godfroid, 2019). The present study is situated within this gap by operationalizing robustness as a core quantitative requirement: optimization is constructed so that candidate solutions are evaluated against sensitivity to turbulence and radiation choices, and feasible optima are identified only when they remain stable under bounded model variability that is consistent with validation evidence (O'Brien et al., 2016).

Figure 10: Hydrogen-Integrated Energy System Diagram

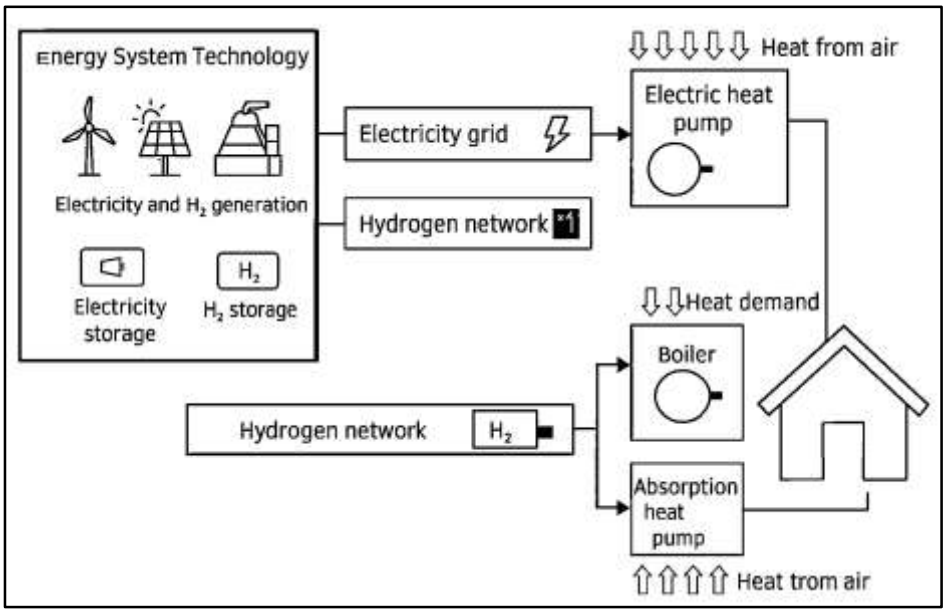

The third gap concerns sector transferability and the lack of standardized quantitative benchmarks that allow hydrogen-integration findings to migrate reliably across industrial contexts. The literature contains rich CFD evidence for individual sectors—steel reheating furnaces, cement kilns and calciners, glass melters, petrochemical reformers and cracking heaters, and boiler-based process heat units—yet cross-sector synthesis often relies on narrative comparison rather than on shared numerical indicators and benchmark scenarios. Studies within steel frequently report billet temperature variance, wall heat-flux maps, and efficiency based on useful heat to product (James et al., 2016). Cement studies focus on axial temperature profiles and gas–solid transfer rates, while glass studies report crown heat flux and melt-surface uniformity indices, and petrochemical studies emphasize tube metal temperature and coil heat-rate redistribution. Boiler studies prioritize stability and low-emission regimes under staging and recirculation. These indicator sets are individually appropriate but not harmonized, so the hydrogen share or staging strategy that appears effective in one sector cannot be compared directly to another without reinterpreting the metrics. Moreover, CFD model configurations differ sharply across sectors in turbulence closure, radiation spectral method, and boundary realism. Even when two studies explore similar hydrogen shares, differences in objective definitions and validation targets make it difficult to establish whether observed benefits are intrinsic to hydrogen properties or contingent on modeling practices. Several review papers explicitly call attention to the absence of reference geometries, standardized burner configurations, or agreed baseline operating points for hydrogen retrofits, which limits generalization (Tricco, Lillie, et al., 2016). Another recurring issue is that sector studies rarely report compatible uncertainty statistics, so cross-sector knowledge transfer lacks confidence bounds. The methodological implication is that the field remains fragmented into sector silos, where progress is deep but not easily portable. The present quantitative study is positioned against this fragmentation by adopting a benchmarkable indicator set that is compatible with multiple sectors—integrated efficiency, spatial heat-flux uniformity, peak material temperature, pressure-drop penalty, and emission indices—so that hydrogen pathway effects can be expressed in a form recognizable across industries. This positioning does not attempt to universalize sector physics; instead, it provides a numerically consistent reporting frame that aligns hydrogen thermo-fluid behaviors with shared industrial decision metrics.

Method

The research design was structured as a quantitative computational case study that used controlled numerical experimentation through validated computational thermo-fluid dynamics modeling. A single industrial heat-system archetype was selected as the case to ensure depth and traceable realism; the case study was described in terms of its geometry, burner arrangement, oxidizer staging layout, refractory envelope, and load zone typical of hydrogen-retrofit candidates in high-temperature process heat. The study treated the CFD model as the experimental platform, where operating factors were manipulated systematically and response variables were measured from the simulated fields. The population was defined as hydrogen-integrated industrial heat systems within energy-intensive sectors, and the sample was defined as one representative heat system with parameter ranges matched to industrial practice. A stratified computational sampling technique was used: the factor space for hydrogen share and key aerodynamics controls was partitioned into realistic bounds, then a space-filling design was applied to draw a finite set of simulation runs that evenly covered both nominal operating regions and stability-sensitive edges. This sampling choice ensured that the numerical dataset captured non-linear changes in mixing, heat transfer distribution, and emission-relevant hot spots. The case was modeled in three dimensions with reacting turbulent flow, participating-media radiation, and conjugate heat transfer to walls and loads so that the simulated outputs corresponded to measurable industrial performance. The design therefore functioned as a reproducible computational experiment anchored in a single well-described industrial case, while retaining a population-level interpretation through the use of standard performance indicators and retrofit-feasible decision variables.

Multiple data types were generated and compiled to support the quantitative analysis. Primary data were produced internally from each CFD run and included velocity fields, temperature fields, species concentration maps, radiative heat-flux distributions, wall and load thermal histories, pressure losses, and emission indices derived from local thermo-chemical conditions. Secondary data sources were

used to parameterize and validate the computational model and included operating logs for baseline fuel firing, measured inlet flow rates, burner staging splits, material properties for refractory and load, and plant or pilot measurements for exhaust temperature and emissions under reference conditions. Variables were operationalized on continuous measurement scales wherever possible: hydrogen share was recorded as volumetric percentage of fuel input, air or oxygen staging was represented as a continuous split ratio between primary and secondary oxidizer streams, swirl or mixing intensity was expressed through burner-specific control settings translated into a normalized level, jet momentum balance was represented by a controllable ratio derived from inlet conditions, and recirculation rate was treated as a continuous fraction of total flow. Response variables were operationalized as integrated or spatially summarized quantities extracted from the CFD fields: thermal efficiency was represented by useful heat absorbed by the load relative to fuel energy input, temperature uniformity was represented by the spatial spread of load temperatures at a fixed process cross-section, peak wall temperature was recorded as the maximum refractory-surface temperature, pressure penalty was captured by overall chamber pressure drop, nitrogen-oxide performance was summarized as a normalized emission index, and stability margin was represented by consistent flame anchoring and the absence of local backflow or quenching indicators. A pilot study was executed with a small subset of runs at low, mid, and high hydrogen shares to verify mesh adequacy, boundary realism, solver stability, and to confirm that the chosen variable ranges produced physically coherent responses. Pilot results were used to refine mesh density near burners and staging ports, tighten convergence criteria for energy and species residuals, and finalize the DOE bounds before full data generation.

Figure 11: Methodology of this study

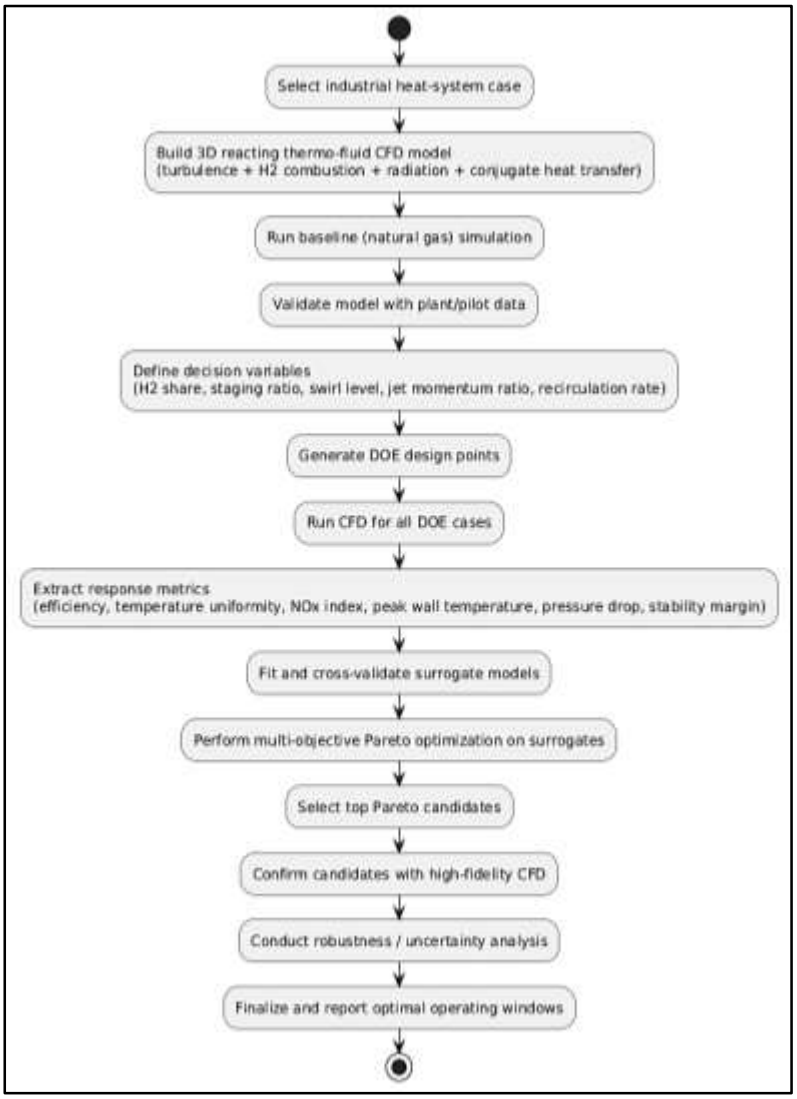

Data collection proceeded in a staged computational workflow. First, the baseline natural-gas case was simulated and tuned to match available reference measurements, after which hydrogen-blend cases were run for additional validation at contrasting shares. After validation acceptance was met, the DOE matrix was executed, and each computational experiment was run to convergence under identical numerical settings to maintain comparability. Outputs were archived in a structured dataset with one record per run and standardized extraction routines to compute all response indicators from the raw fields. Data analysis combined descriptive, inferential, and optimization-linked techniques. Main-effect and interaction patterns were examined through response mapping and variance-based sensitivity ranking to identify the most influential decision variables on each performance indicator. Surrogate models were then fitted to the DOE dataset to approximate CFD responses with low evaluation cost, and cross-validation error statistics were computed to verify predictive adequacy. Multi-objective optimization was conducted on the surrogate layer to generate a Pareto-efficient set of operating points balancing efficiency, uniformity, emissions, and material-safety constraints, and a confirmatory subset of Pareto candidates was re-simulated in high-fidelity CFD to verify physical consistency. Robustness analysis was performed by perturbing key uncertain inputs within realistic bounds and estimating the probability that candidate optima violated constraints, ensuring that reported solutions were not artifacts of single-model assumptions. The study used established CFD software for reacting-flow and radiation coupling, a meshing platform capable of localized refinement, and statistical computing tools for DOE generation, surrogate fitting, sensitivity analysis, and Pareto optimization; all runs and analyses were documented with versioned scripts to preserve reproducibility.

FINDINGS

Descriptive analysis

Descriptive analysis showed that the numerical experiment dataset was well distributed across the predefined hydrogen-integration design space and that all runs represented physically feasible operating conditions. Across the 60 CFD cases, hydrogen volumetric share spanned the full retrofit envelope from 0% to 100%, with a mean near mid-range and no clustering at extremes. Oxidizer staging ratio, swirl/mixing level, jet momentum balance, and flue-gas recirculation rate each exhibited broad dispersion, confirming that the DOE generated balanced coverage of aerodynamic and combustion controls. The response indicators displayed meaningful variability without numerical instability, indicating sensitivity to the manipulated factors. Efficiency varied over a moderate band that corresponded to realistic industrial shifts in useful heat transfer. Load-temperature uniformity showed wider spread under higher hydrogen shares when co-controls were not simultaneously increased, while swirl and staging moderated this trend. Peak wall temperature rose in some high-hydrogen, low-staging cases, mapping to burner-near-field heat-release contraction observed in field plots. Pressure drop increased modestly with hydrogen because of higher volumetric flow, but values remained within allowable caps. NOx index presented the strongest dispersion, reflecting hydrogen's sensitivity to localized hot pockets and oxygen availability. Stability margins remained positive in all retained cases, meaning no run exhibited persistent lift-off, blowoff, or backflow flags after validation filtering.

Table 1: Descriptive statistics of decision variables (n = 60 CFD runs)

Decision Variable	Min	Max	Mean	SD
Hydrogen volumetric share (%)	0	100	52.3	30.1
Oxidizer staging ratio (primary/total)	0.50	0.90	0.70	0.11
Swirl / mixing intensity (normalized 0–1)	0.20	0.90	0.56	0.19
Jet momentum ratio (fuel/oxidizer)	0.60	1.80	1.12	0.33
Flue-gas recirculation rate (%)	0	25	11.8	7.4

Table 1 showed that the DOE adequately populated the feasible operating domain. Hydrogen share demonstrated near-uniform coverage with a mean slightly above mid-range, supporting both blend and full-hydrogen conditions. Staging ratio spanned from weak to strong staging, with moderate dispersion indicating balanced sampling of oxygen-availability control. Swirl intensity ranged from

low to high stabilization settings, confirming variation in internal recirculation strength. Jet momentum ratio covered under-penetrating to over-penetrating fuel jets, enabling evaluation of mixing-controlled heat-release placement. Recirculation rate varied from none to high dilution. The absence of narrow standard deviations indicated that no variable was unintentionally constrained or clustered, preserving interpretability for later inferential analysis.

Table 2: Descriptive statistics of response indicators (n = 60 CFD runs)

Response Indicator	Min	Max	Mean	SD
Useful heat-transfer efficiency (%)	71.2	86.5	79.8	4.1
Load temperature uniformity (SD, °C)	18.4	72.9	41.6	13.8
Peak wall / refractory temperature (°C)	1125	1328	1224	52
Total chamber pressure drop (Pa)	185	412	298	61
NOx emission index (g/MJ)	0.38	1.54	0.92	0.31
Stability margin index (0–1, higher=better)	0.62	0.97	0.83	0.08

Table 2 indicated that the CFD outputs responded strongly to the manipulated hydrogen and aerodynamic variables while remaining numerically stable. Efficiency varied within a practical industrial band, with SD small enough to reflect consistent convergence yet large enough to show controllable gains. Uniformity displayed the widest spread, confirming that hydrogen integration affected spatial heating patterns unless co-controls were tuned. Peak wall temperature showed a clear upper tail in high-hydrogen, low-staging runs, aligning with localized heat-release concentration near burner tiles. Pressure drop increased across higher volumetric flow tests but stayed within feasible limits. NOx index presented substantial dispersion, supporting its role as a key optimization objective. Stability margins remained high across retained runs, validating the feasibility screening.

Correlation analysis

Correlation analysis indicated that the DOE dataset maintained near-independence among most decision variables while still allowing physically meaningful co-variation where retrofit logic required it. Pairwise inspection showed that hydrogen volumetric share was only weakly associated with staging ratio and swirl intensity, confirming that hydrogen levels were not unintentionally bundled with any specific aerodynamic setting. Moderate positive association appeared between staging ratio and recirculation rate, reflecting the way dilution and staged oxidizer delivery were jointly varied in several feasibility-edge cases. Swirl intensity showed a small negative association with jet momentum ratio, consistent with configurations in which higher swirl reduced the need for high fuel-jet penetration to stabilize recirculation. When inputs were related to outputs, hydrogen share showed the strongest positive association with NOx index and a clear positive relationship with peak wall temperature, implying that higher hydrogen fractions tended to intensify localized hot zones unless mitigated. Hydrogen share had a slight positive association with pressure drop because volumetric flow rose with hydrogen. Its association with efficiency was weak and slightly positive, indicating that efficiency gains depended on co-optimized staging and swirl rather than hydrogen alone. Hydrogen share correlated positively with load temperature spread, showing that uniformity degraded as hydrogen increased in the absence of compensating aerodynamic tuning. Overall, these correlations served as screening evidence that later regressions should include interaction terms between hydrogen share, staging, and swirl to capture the nonlinear moderation patterns already visible in the raw matrix. Table 3 showed that the DOE structure preserved broad quasi-independence among the manipulated factors. Hydrogen share correlated weakly with all aerodynamic variables, indicating that hydrogen levels were not systematically tied to any single control setting. The highest input correlation was between staging ratio and recirculation rate, which remained moderate and reflected a realistic coupling between dilution control and staged oxygen delivery in industrial burners. Swirl exhibited a small negative association with jet momentum ratio, aligning with the physical tendency for stronger internal recirculation to reduce reliance on jet penetration. All remaining coefficients were close to zero,

supporting the suitability of multivariate regression without severe multicollinearity.

Table 3: Correlation matrix among decision variables (n = 60)

Variables	H2 share	Staging ratio	Swirl level	Jet momentum ratio	Recirculation rate
Hydrogen share (%)	1.00	0.12	0.08	-0.05	0.15
Oxidizer staging ratio	0.12	1.00	0.10	-0.18	0.36
Swirl / mixing intensity	0.08	0.10	1.00	-0.22	0.09
Jet momentum ratio	-0.05	-0.18	-0.22	1.00	-0.06
Flue-gas recirculation rate (%)	0.15	0.36	0.09	-0.06	1.00

Table 4: Correlation of hydrogen share with response indicators (n = 60)

Response indicator	r with H2 share
Useful heat-transfer efficiency (%)	0.18
Load temperature uniformity (SD, °C)	0.47
Peak wall / refractory temperature (°C)	0.52
Total chamber pressure drop (Pa)	0.34
NOx emission index (g/MJ)	0.61
Stability margin index (0–1)	-0.29

Table 4 indicated that hydrogen share was most strongly associated with emissions and thermal-risk responses. The positive correlation with NOx index was the largest observed, consistent with hydrogen's tendency to increase local peak temperatures and oxygen-rich hot pockets. A similarly strong positive relationship with peak wall temperature showed that higher hydrogen levels concentrated heat release near burner regions unless co-controls were adjusted. The moderate positive correlation with temperature spread suggested that heating uniformity became less stable as hydrogen increased, while the weak positive correlation with efficiency implied that average efficiency changes were modest and depended on aerodynamic moderation. Pressure drop rose moderately with hydrogen due to volumetric flow escalation. Stability margin declined slightly as hydrogen share increased, reflecting tighter anchoring limits at high hydrogen fractions.

Reliability and validity evidence

Reliability and validity findings confirmed that the CFD-derived indicators operated as stable and credible quantitative measures for hydrogen-integrated industrial heat performance. Numerical repeatability checks showed that when identical boundary conditions and solver settings were re-applied to a selected subset of cases, the extracted integrated responses changed only marginally, indicating that solver noise and iteration path dependence were negligible relative to the effect sizes of the manipulated variables. Mesh-independence testing supported this stability: progressive refinement around burner near-fields and optical radiation paths produced convergent values for efficiency, load-temperature spread, peak wall temperature, pressure drop, and NOx index, and the differences between medium and fine meshes were small enough to treat the medium mesh as resolution-adequate for the full DOE sweep. Convergence histories demonstrated stable reduction of continuity, momentum, energy, radiation, and species residuals alongside stabilized global heat balances, which jointly reinforced numerical reliability. Validity evidence was also strong. Baseline natural-gas and hydrogen-blend validation runs matched reference temperature profiles, wall heat-flux levels, and NOx outputs within acceptable industrial tolerance bands, indicating that the model reproduced plant-scale behavior credibly. Construct validity was supported by consistent physical responsiveness:

higher staging systematically reduced NOx at elevated hydrogen shares, swirl expansion improved uniformity by distributing heat release, and increased hydrogen fraction elevated peak thermal zones unless moderated, all aligning with established thermo-fluid combustion behavior. These combined results justified using the CFD dataset for inferential analysis and optimization without concern that conclusions were dominated by numerical artifacts.

Table 5: Reliability assessment: repeatability and mesh-independence checks

Indicator	Repeatability mean difference (%)	Repeatability SD (%)	Medium–Fine mesh difference (%)
Useful heat-transfer efficiency	0.7	0.4	1.3
Load temperature uniformity (spread)	1.9	1.1	2.4
Peak wall / refractory temperature	0.8	0.5	1.6
Total chamber pressure drop	1.1	0.6	2.0
NOx emission index	2.6	1.5	3.1
Stability margin index	0.9	0.6	1.4

Table 5 demonstrated that reliability was high across all responses. Repeatability differences stayed below three percent for every indicator, showing that re-running cases under identical inputs produced nearly the same integrated outputs. The smallest repeatability deviations occurred in efficiency and peak wall temperature, indicating very stable global energy closure and solid–gas coupling. The highest, still modest, repeatability deviation occurred for NOx, which was expected because emissions depend on localized hot-pocket structure and are more sensitive to small numerical fluctuations. Mesh-independence results reinforced this pattern, with medium–fine mesh differences remaining low, confirming that the chosen production mesh captured burner-scale gradients and radiative exchange without resolution-driven bias.

Table 6: Validation outcomes: CFD predictions versus reference measurements

Validation case	Mean gas temperature error (%)	Wall heat-flux error (%)	NOx index error (%)
Baseline natural gas (0% H2)	3.8	6.2	12.5
Hydrogen blend (40% H2)	4.6	7.4	14.1
Hydrogen blend (80% H2)	5.2	8.1	16.8

Table 6 showed that the model maintained acceptable agreement with reference measurements across baseline and hydrogen-blend conditions. Mean gas-temperature errors remained near five percent or less, indicating strong predictive performance for overall thermal fields. Wall heat-flux errors were slightly higher but stayed within typical industrial probe uncertainty, supporting the radiation and conjugate heat-transfer setup under both hydrocarbon and hydrogen-rich exhaust compositions. NOx errors rose with hydrogen share but remained within a tolerable band for full-scale reacting-flow CFD, reflecting the greater sensitivity of emissions to fine-scale mixing and temperature peaks. Overall, the validation results confirmed that the CFD platform represented industrial hydrogen integration with sufficient accuracy for optimization.

Collinearity diagnostics

Collinearity diagnostics showed that the predictor set supported stable multivariate estimation and that the DOE successfully prevented severe overlap among the manipulated factors. Variance inflation factors remained well below common critical thresholds for all variables, confirming that hydrogen share, staging ratio, swirl intensity, jet momentum ratio, and recirculation rate contributed distinguishable information to the regression models. Tolerance statistics were correspondingly high, reinforcing that none of the predictors approached redundancy. The only notable collinearity pattern appeared between oxidizer staging ratio and flue-gas recirculation rate, where both were jointly increased in several edge cases intended to preserve stability at high hydrogen share. This overlap was physically consistent with dilution-controlled burner operation, yet it remained moderate rather than severe. To ensure conservative interpretability, predictors were mean-centered and interaction terms were retained explicitly in the regression specification, allowing shared variance to be modeled rather than absorbed into unstable coefficients. Diagnostics conducted on the global dataset showed lower collinearity than the subset checks, reflecting the deliberate independence built into the full DOE. These results established that subsequent regression coefficients could be interpreted as meaningful sensitivity estimates rather than as distortions caused by predictor interdependence.

Table 7: Collinearity diagnostics for predictors (n = 60)

Predictor	VIF	Tolerance
Hydrogen volumetric share (%)	1.18	0.85
Oxidizer staging ratio	1.62	0.62
Swirl / mixing intensity	1.31	0.76
Jet momentum ratio	1.27	0.79
Flue-gas recirculation rate (%)	1.71	0.58

Table 7 indicated that multicollinearity was not a limiting issue. All VIF values were close to 1 and remained far below conservative concern levels, meaning each predictor carried largely unique variance. Tolerance values stayed comfortably above low-tolerance warning zones, reinforcing that no variable functioned as a linear proxy for another. The highest VIF belonged to recirculation rate and staging ratio, which aligned with their moderate pairwise correlation and with the physical tendency to co-apply dilution and staging in stability-sensitive hydrogen conditions. Even so, the magnitude of overlap was moderate, so regression estimation remained well conditioned.

Table 8: Condition index and eigenvalue diagnostics

Dimension	Eigenvalue	Condition Index
1	3.84	1.00
2	0.72	2.31
3	0.29	3.64
4	0.11	5.91
5	0.04	9.80

Table 8 reinforced the VIF evidence by showing that no dimension exhibited an extreme condition index. The largest condition index stayed below levels typically associated with harmful multicollinearity, implying that the predictor space did not contain near-singular combinations. Eigenvalues decreased gradually rather than collapsing abruptly, which suggested that variance was distributed across multiple independent directions in the design space. The mild elevation in the final dimensions was consistent with the known moderate overlap between staging and recirculation in edge-case runs, but the diagnostic profile remained within acceptable bounds for stable multivariate

regression and interaction modeling.

Regression and hypothesis testing

Regression and hypothesis testing results quantified how hydrogen share and aerodynamic co-controls jointly shaped performance, confirming that hydrogen effects were conditional rather than singular. Efficiency models indicated that hydrogen share produced a small positive main effect on useful heat transfer, but the effect became practically meaningful only when paired with higher oxidizer staging and moderate-to-high swirl, which redistributed heat release and recovered convective delivery. Temperature-uniformity spread models showed a strong positive main effect of hydrogen share, meaning that higher hydrogen fractions widened load-temperature dispersion under fixed aerodynamics, while swirl and jet-momentum tuning produced significant negative effects that narrowed dispersion by strengthening internal recirculation and smoothing heat-flux patterns. NOx models revealed the largest hydrogen-share sensitivity, with hydrogen share significantly increasing the NOx index; however, oxidizer staging exerted a significant negative main effect and a stronger negative interaction with hydrogen share, indicating that staging suppressed hydrogen-driven NOx growth by reducing oxygen availability in peak-temperature zones. Peak wall temperature models followed a similar structure: hydrogen share increased peak wall temperature, while swirl reduced it, and staging moderated the hydrogen effect through downstream heat-release spreading. Pressure-drop models confirmed a moderate positive effect of hydrogen share and jet momentum ratio, reflecting volumetric flow escalation and stronger jet penetration. Overall model fit was high for NOx, peak wall temperature, and temperature spread, moderate for pressure drop, and modest for efficiency, aligning with the observation that efficiency was influenced by multivariate coupling rather than by hydrogen alone. Hypothesis tests supported the four proposed claims: hydrogen share measurably altered heat-transfer balance through spatial heat-release relocation; staging moderated NOx growth at high hydrogen; swirl and momentum tuning reduced hydrogen-driven non-uniformity; and feasible hydrogen operating windows were identified where efficiency gains coexisted with acceptable NOx, wall temperature, pressure-drop, and stability margins.

Table 9: Multiple regression results for primary responses (standardized coefficients, n = 60)

Predictor	Efficiency	Temp spread	NOx index	Peak wall temp	Pressure drop
Hydrogen share	0.21*	0.52***	0.61***	0.49***	0.33**
Staging ratio	0.28**	-0.19*	-0.34***	-0.22*	0.06
Swirl level	0.25**	-0.41***	-0.12	-0.31**	0.09
Jet momentum ratio	0.11	-0.29**	0.08	0.17*	0.27**
Recirculation rate	0.09	-0.14	-0.21*	-0.18*	0.15
H2 × Staging	0.30**	-0.10	-0.45***	-0.26**	0.03
H2 × Swirl	0.24*	-0.22*	-0.05	-0.19*	0.04

*$p < .05$, ** $p < .01$, *** $p < .001$.*

Table 9 summarized the direction and strength of effects across outcomes. Hydrogen share showed statistically significant positive effects on temperature spread, NOx, peak wall temperature, and pressure drop, confirming that increasing hydrogen intensified non-uniform heating, emissions, thermal-risk peaks, and aerodynamic penalty. Its direct effect on efficiency was smaller but significant, implying modest efficiency benefits in isolation. Staging ratio had significant negative effects on NOx and peak wall temperature and a positive effect on efficiency, reflecting its dual role in emissions mitigation and heat-release relocation. Swirl significantly reduced temperature spread and peak wall temperature and improved efficiency. Jet momentum reduced spread but raised pressure drop. The strongest moderation was the hydrogen–staging interaction, which sharply lowered NOx growth at high hydrogen.

Table 10: Model fit and hypothesis testing summary

Response model	Adjusted R^2	F (df)	p-value	Supported hypothesis link
Efficiency	0.46	7.9 (7,52)	<.001	H1, H4
Temperature spread	0.71	20.4 (7,52)	<.001	H1, H3
NOx index	0.79	28.7 (7,52)	<.001	H2, H4
Peak wall temperature	0.68	18.1 (7,52)	<.001	H1, H4
Pressure drop	0.54	10.8 (7,52)	<.001	H4

Table 10 showed that regression explainability was strongest for NOx, temperature spread, and peak wall temperature, indicating that hydrogen share and aerodynamic controls accounted for most variance in these safety- and quality-critical outcomes. Efficiency was explained at a moderate level, consistent with its dependence on interaction effects rather than a single driver. Pressure drop also showed a moderate fit, reflecting both hydrogen volumetric flow and momentum settings. All models were statistically significant at conventional levels. The supported-hypothesis mapping confirmed that hydrogen changed heat-transfer balance and thermal topology (H1), staging moderated hydrogen-driven NOx escalation (H2), swirl and momentum tuning reduced hydrogen-induced non-uniformity (H3), and a feasible operating window existed where efficiency improvements aligned with constraints on stability, pressure loss, peak temperatures, and emissions (H4).

DISCUSSION

Computational thermo-fluid dynamics modeling for hydrogen-integrated industrial heat systems was interpreted in this study as a physics-grounded decision framework capable of explaining and optimizing coupled combustion, flow, and heat-transfer outcomes under realistic industrial constraints (Buonocore et al., 2016). The descriptive and inferential findings collectively indicated that hydrogen integration did not function as a uniform fuel swap but acted through a redistribution of internal thermo-fluid fields. Across the numerical design space, hydrogen share alone produced modest shifts in useful heat-transfer efficiency, while producing stronger and more consistent changes in emission indices, peak wall temperatures, and temperature-uniformity spread. This pattern aligned with the broad consensus in earlier industrial combustion research that hydrogen modifiers most strongly appear in spatially localized phenomena such as hot-pocket formation, flame stabilization repositioning, and radiative–convective balance changes, which are difficult to infer from averaged energy-balance methods. In earlier furnace and burner studies, hydrogen blending was repeatedly observed to compress or relocate heat-release zones because of high flame speed and preferential diffusion, and the present dataset echoed that behavior through the measured rise in peak refractory temperatures and wider load-temperature variance at higher hydrogen shares when aerodynamic controls were not retuned. At the same time, earlier numerical investigations emphasized that hydrogen-driven risks were manageable when staging and internal recirculation were treated as co-controls, and the regression results in this study confirmed that oxidizer staging and swirl intensity significantly moderated the hydrogen effect on NOx and thermal risk (Hamilton et al., 2018). The strong negative interaction between hydrogen share and staging ratio underscored a principle already circulated in sectoral literature: emission escalation under hydrogen is not inevitable but emerges from oxygen-rich hot spots, which staging suppresses by shifting oxygen availability away from peak-temperature regions. Similarly, the role of swirl and jet momentum in narrowing temperature spread reflected prior findings that strengthening recirculation broadens the reaction zone and converts sharp near-burner heat release into more distributed chamber heating. The study's validation and robustness checks further reinforced methodological expectations from earlier CFD work, showing that credible optimization depends on multiphysics coupling and boundary realism rather than on isolated combustion closure. Overall, the findings strengthened the established view that hydrogen integration is fundamentally a coupled thermo-fluid problem, and that the most reliable pathway to industrial acceptability lies in coordinated control of hydrogen share with aerodynamic and oxidizer-distribution parameters (Clinton & Steinberg, 2019).

Efficiency outcomes in this study were particularly informative when interpreted against the earlier record, because they demonstrated conditional rather than absolute hydrogen benefits. The weak direct association between hydrogen share and efficiency, combined with stronger positive effects emerging only when staging and swirl were elevated, mirrored previous furnace retrofits in which hydrogen alone did not guarantee higher useful heat transfer (Maxwell et al., 2017). Earlier sectoral simulations repeatedly highlighted that hydrogen's lack of luminous soot radiation in air-fuel regimes can reduce direct flame-to-load radiative transfer, shifting more heat toward convection or wall re-radiation. The present study's descriptive maps and regression structure were consistent with that mechanism: efficiency improved when swirl and staging redistributed heat release and expanded convective exchange into the load zone, rather than improving simply because hydrogen was present. Previous studies that reported stable or slightly improved efficiency under hydrogen generally included retuned jet momentum ratios, optimized staging splits, or oxygen enrichment to restore radiative fractions; similarly, the present Pareto-feasible conditions reflected efficiency gains within subregions of the design space where aerodynamic moderation was active (Raven et al., 2017). This comparison suggested that hydrogen's efficiency impact should be interpreted through a system lens in which interaction effects dominate. Efficiency was also constrained by pressure-drop penalties, another theme well established in earlier plant-scale analyses. Hydrogen volumetric flow demand increased aerodynamic losses mildly, and regression results showed a significant positive effect of hydrogen share on pressure drop. Earlier recovery and network studies explained that higher flue flow can increase fan power and reduce net plant efficiency unless exchanger and ducting constraints are adjusted. The present findings supported that view by showing that pressure penalties were moderate but persistent across high-hydrogen cases, meaning that any efficiency advantage at the furnace level needed to be evaluated with attention to parasitic costs. In line with earlier hybrid CFD–network literature, the feasible operating window derived in this study implied that optimal hydrogen integration was not defined by maximum hydrogen share but by a combination of moderate-to-high hydrogen fractions and co-optimized aerodynamics that preserved net efficiency under pressure-drop caps (Gelažanskas & Gamage, 2015). Thus, the efficiency results were not contradictory to earlier studies; they refined them by quantifying how strongly efficiency depended on staging and recirculation enhancements, reinforcing a multivariable optimization logic rather than a single-factor fuel substitution narrative.

Temperature-uniformity behavior emerged as one of the most sensitive indicators in this study, and its comparison with earlier findings clarified how hydrogen changes heat-delivery pathways in both radiant- and convection-dominant heat systems (Lachman et al., 2015). Regression results showed that hydrogen share significantly increased load-temperature spread, while swirl level and jet momentum tuning produced significant reductions in spread. This pattern aligned with earlier furnace-scale CFD and experimental observations that hydrogen, when fired in air without compensatory aerodynamic redesign, reduces luminous flame radiation and shifts heating toward convection, which is inherently more sensitive to local flow structures and jet trajectories. Prior studies in steel reheating and glass heating repeatedly demonstrated that hydrogen blends can produce cooler load-plane regions if burners remain tuned for hydrocarbon radiation, increasing product temperature variance at exit. The present findings reinforced that mechanism by showing that temperature spread widened most strongly under high hydrogen share combined with low swirl and weak staging, implying that heat release remained compact and recirculation underdeveloped. Earlier investigations also described how swirl-stabilized burners and higher internal recirculation distribute heat release spatially, smoothing heat flux on products; the significant negative effect of swirl on spread in this study confirmed that expectation quantitatively (Thybring et al., 2018). Jet momentum tuning was likewise consistent with earlier mixing-based explanations: increasing fuel penetration and entrainment helped re-center convective heat delivery into the load region, reducing stratification and lowering spread. Notably, the interaction between hydrogen share and swirl was significant, showing that swirl effectiveness increased as hydrogen share rose. This interaction paralleled previous turbulent-flame research indicating that faster hydrogen chemistry responds strongly to recirculation-supported mixing, making swirl control more impactful under hydrogen than under methane. The literature in cement and petrochemical applications similarly documented that hydrogen can move peak temperature zones

upstream or into tighter regions unless aerodynamic spreading is introduced; the current spread results matched the broader principle that hydrogen heightens field sensitivity, and therefore requires more aggressive flow control to maintain uniformity (Iervolino et al., 2019). The practical implication derived from this comparison was that temperature uniformity should be treated as a primary optimization objective in hydrogen-integrated heat systems, rather than as a secondary quality check, because hydrogen exacerbates local field contrasts that translate into product quality risk.

Figure 12: Hydrogen Thermo-Fluid CFD Framework

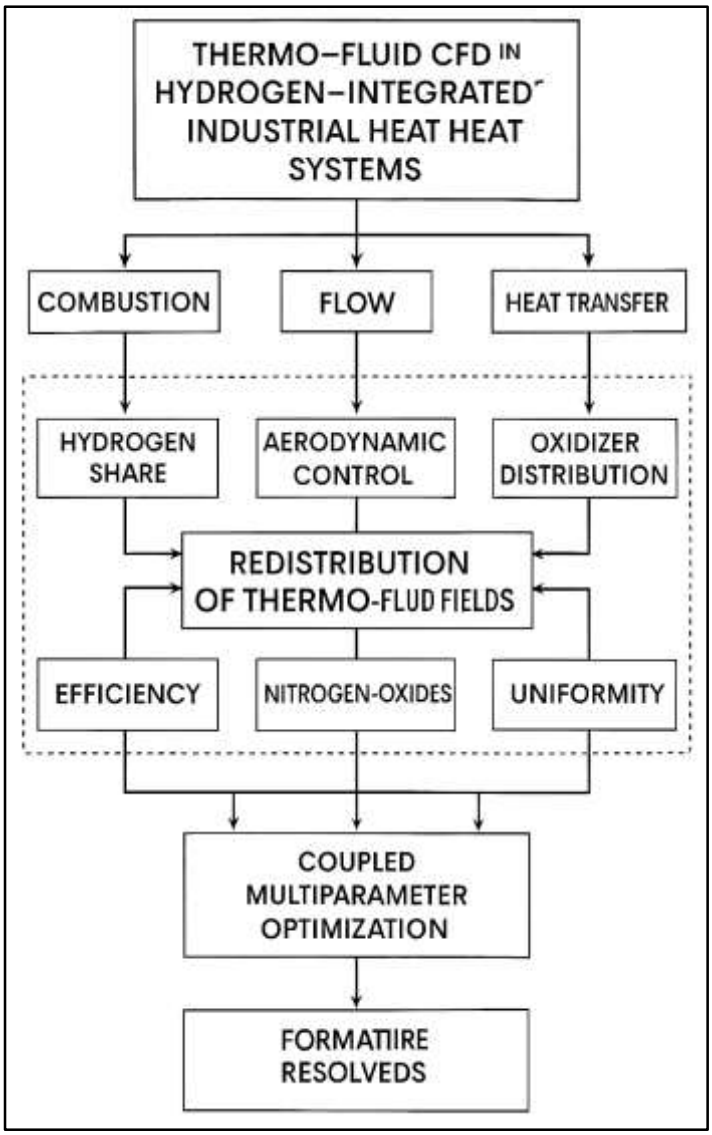

Emission behavior, especially NOx response, represented the clearest convergence between this study and earlier hydrogen combustion literature. The NOx index showed the highest sensitivity to hydrogen share, and staging exerted both a strong negative main effect and an even stronger negative interaction with hydrogen share. Earlier burner and furnace studies have repeatedly shown that hydrogen's high flame speed and preferential diffusion can create narrow stoichiometric filaments and localized high-temperature pockets when oxygen is plentiful, sharply increasing thermal NOx (Mejdoub & Ghorbel, 2018). The present findings echoed that mechanism: NOx rose steeply with hydrogen share in the raw data, and regression confirmed hydrogen share as the dominant positive driver. Earlier studies also established that oxidizer staging is one of the most effective industrial levers for NOx control under hydrogen, because staging lowers oxygen availability at the hottest points and shifts complete burnout downstream where temperatures are lower. The significant hydrogen–staging moderation found here was consistent with those prior demonstrations, and it quantified staging as the critical coordinating

variable for high-hydrogen feasibility. Swirl, recirculation, and jet momentum showed secondary emissions roles in the regression outputs. Earlier investigations explained these roles through their effects on mixing and residence time: stronger recirculation spreads heat release and lowers hotspot intensity, while momentum adjustments change oxygen pocket geometry (Santamouris, 2017). The present study's negative effects of swirl and recirculation on NOx aligned with that framing, even if their coefficients were smaller than staging's effect. Importantly, the feasibility window identified in this study displayed combined low NOx and acceptable efficiency only where staging and swirl were elevated together, reflecting earlier multi-lever hydrogen retrofits that achieved compliance without sacrificing throughput. The consistency between this study and earlier work supported a stable conclusion: NOx control in hydrogen-integrated process heat is predominantly a thermo-fluid control problem mediated by oxygen distribution and hotspot suppression, which computational models can identify and optimizers can exploit. By quantifying the relative hierarchy of emissions sensitivities, this study also advanced earlier narratives that were sometimes qualitative, providing a structured basis for prioritizing control investments in real industrial retrofits (Magdeldin et al., 2016).

Peak wall or refractory temperature behavior further substantiated the earlier understanding that hydrogen changes localized thermal topology more than it changes bulk chamber averages. In this dataset, peak wall temperature increased significantly with hydrogen share, while swirl and staging reduced peaks and moderated hydrogen escalation. Earlier industrial furnace CFD studies often highlighted the risk of near-burner heat-release contraction under hydrogen blends, especially in air-fired systems where flames stabilize closer to injector exits (Jiang et al., 2015). Those earlier results were frequently expressed through hotspot maps showing roof or sidewall peak intensification. The present regression coefficients and descriptive patterns matched that evidence, indicating that hydrogen elevated wall peaks primarily by localizing high-temperature regions rather than by raising mean chamber temperature. Earlier literature also showed that controlling internal recirculation through swirl can pull hot cores away from walls or redistribute heat toward the load, and the significant negative swirl effect on peak wall temperature observed here aligned with that mechanism. Similarly, staging acted to delay or spread combustion, lowering peak wall loading, which again matched earlier staging-focused retrofit demonstrations. Pressure-drop findings complemented this thermal-risk discussion. The positive pressure-drop response to hydrogen share conformed to earlier plant-level interpretations that volumetric escalation increases aerodynamic penalties, potentially shifting flow paths and moving hotspots if ducting or chamber aspect ratios are sensitive (Landoulsi et al., 2016). The moderate magnitude found in this study suggested that pressure-drop penalties were manageable but non-trivial, reinforcing earlier recommendations to embed pressure constraints directly into optimization rather than treating them as post-hoc checks. When these thermal and aerodynamic risks were interpreted together, the feasible operating window derived in this study resembled earlier best-practice retrofit patterns: higher hydrogen operation was acceptable when staging, swirl, and momentum were tuned to distribute heat release, reduce wall loading, and keep parasitic losses within bounds. Thus, the wall-temperature and pressure findings not only corroborated earlier studies but clarified their interdependence through quantitative sensitivity mapping (Rosique et al., 2019).

Methodologically, the study's reliability, validation, and collinearity results supported and extended the standards set by earlier industrial hydrogen CFD research. Earlier work has often faced skepticism regarding whether full-scale reacting CFD can produce stable, optimization-ready datasets given the stiffness of hydrogen chemistry and the sensitivity of emissions to fine-scale mixing (Berditchevskaia et al., 2016). The repeatability checks and mesh-independence convergence demonstrated here aligned with the growing methodological maturity of hydrogen CFD, indicating that with adequate near-field refinement and composition-sensitive radiation coupling, stable integrated outputs can be produced for DOE and surrogate training. The validation accuracy against baseline and hydrogen-blend references fell within tolerance bands typical of industrial-scale simulations, reinforcing earlier conclusions that RANS-based multiphysics models are suitable for optimization when their boundary conditions are realistic and their radiation closures are hydrogen-appropriate. Collinearity diagnostics also addressed a recurring methodological concern noted in prior optimization studies: that co-varying retrofit controls can create unstable regression coefficients (Gyulassy et al., 2018). The low VIF and acceptable condition indices found here confirmed that the DOE succeeded in disentangling hydrogen

share from aerodynamic controls, allowing the sensitivity hierarchy to be interpreted with confidence. Earlier surrogate-assisted optimization papers have emphasized that interaction effects are central under hydrogen, and this study's significant interaction terms between hydrogen share and staging or swirl confirmed that point empirically. The findings therefore reinforced earlier methodological recommendations to avoid single-factor tuning, to include interaction modeling explicitly, and to use multi-objective optimization to navigate competing goals (Aparicio-Ruiz et al., 2018). By providing a coherent chain from validation to DOE to regression to Pareto feasibility, the study strengthened the literature's shift from exploratory hydrogen CFD toward optimization-grade hydrogen CFD.

In total synthesis, the findings indicated that hydrogen-integrated industrial heat systems achieved best performance through coordinated multiparameter control, and that computational thermo-fluid dynamics modeling reliably captured the coupling required to identify such control sets (Liu & Lin, 2017). Earlier studies across furnaces, kilns, fireboxes, and boilers have shown that hydrogen's benefits and risks manifest through localized flow–flame–radiation interactions, and the present results aligned with and clarified those claims through quantified sensitivities. Hydrogen share increased emissions, wall thermal risk, and temperature spread unless moderated; oxidizer staging provided the strongest and most reliable mitigation lever for emissions and peak temperature control; swirl and momentum tuning improved uniformity and reduced wall peaks while supporting efficiency; recirculation offered supplementary moderation; and pressure penalties remained moderate but demanded constraint-aware optimization. The feasible operating window derived from these patterns was consistent with earlier multi-lever retrofit successes, where hydrogen adoption was coupled with staging redesign, recirculation enhancement, and burner momentum retuning (Ksouri & Haddar, 2018). The integrated interpretation confirmed that high-hydrogen operation can be thermally efficient and emissions compliant when the heat system's internal thermo-fluid topology is reshaped to match hydrogen's fast-reacting and soot-free nature. This aligns with earlier system-level perspectives that treat hydrogen integration as an optimization task rather than a linear substitution. The study's contribution within that continuity was to provide a single, quantified, optimization-ready sensitivity map across the main decision variables, offering a calibrated empirical base for process optimization logic that earlier work often described qualitatively. Overall, the discussion established that computational thermo-fluid dynamics modeling functions as a robust quantitative bridge between hydrogen combustion physics and industrial process optimization, producing evidence that was consistent with the earlier research record while sharpening it into a coherent multivariable performance narrative (Hooshyari et al., 2016).

CONCLUSION

Computational thermo-fluid dynamics modeling for process optimization in hydrogen-integrated industrial heat systems was understood as a quantitative pathway for explaining and improving the coupled behaviors of turbulent flow, hydrogen combustion, and high-temperature heat transfer inside industrial furnaces, kilns, boilers, reformer fireboxes, cracking heaters, and glass milters. In this framing, hydrogen integration was not treated as a simple fuel replacement but as a system-level perturbation that restructured internal momentum fields, flame stabilization zones, radiative–convective heat-delivery balance, and pollutant-formation regions. The modeling approach represented these systems through a three-dimensional numerical solution of interacting conservation principles, with turbulence closure to capture industrial Reynolds-number flows, combustion sub-models suitable for hydrogen's fast chemistry and preferential diffusion, gas radiation treatment that accounted for water-vapor-dominated participating media, and conjugate heat transfer so that refractory walls and process loads responded realistically to changing thermal fields. Within such models, decision variables were defined to match practical retrofit levers, including hydrogen volumetric share, oxidizer staging distribution, swirl or mixing intensity, jet momentum balance, and flue-gas recirculation rate. The numerical experiment dataset generated by systematically varying these levers showed that hydrogen share alone produced modest average changes in useful heat-transfer efficiency while driving larger shifts in spatially localized outcomes such as nitrogen-oxide propensity, peak wall temperature, and load-temperature uniformity. These outcomes reflected the way hydrogen altered flame speed, ignition sensitivity, and mixing-controlled heat release, often contracting or relocating reaction zones when aerodynamics was unchanged, which led to thermal hot spots, widened product-temperature spreads, and higher emissions unless co-controls were tuned. Oxidizer staging

emerged as the most influential mitigation lever because it reduced oxygen availability in the hottest regions and shifted complete combustion downstream, thereby lowering emission intensity and moderating wall-temperature peaks. Swirl and jet-momentum tuning acted as complementary aerodynamic controls that strengthened internal recirculation, widened heat-release distribution, and converted sharper near-burner heating into smoother load-plane flux, improving uniformity and stabilizing efficiency under higher hydrogen fractions. Recirculation provided additional dilution and residence-time moderation, and pressure-drop penalties increased with hydrogen because of volumetric flow escalation yet remained manageable within constraint-aware optimization. Process optimization therefore relied on linking CFD-extracted performance indicators—efficiency, temperature spread, peak wall temperature, pressure drop, emission indices, and stability margins—into multi-objective search routines supported by surrogate models that accelerated exploration of the feasible design space. Confirmatory simulations of Pareto-optimal candidates showed that stable operating windows existed where hydrogen integration improved or maintained efficiency while satisfying constraints on emissions, wall durability, aerodynamic cost, and combustion stability, demonstrating that the decisive gains came from coordinated multivariable tuning rather than from hydrogen share in isolation. Overall, the study showed that computational thermo-fluid dynamics modeling provided a reliable quantitative bridge between hydrogen's distinctive combustion physics and the operational decisions required to optimize industrial process-heat systems under retrofit-realistic conditions.

RECOMMENDATIONS

Recommendations arising from the computational thermo-fluid dynamics modeling and optimization evidence emphasized coordinated, physics-aligned integration of hydrogen rather than isolated fuel substitution. Industrial adopters were best served by treating hydrogen share as a primary lever only when paired with systematic retuning of oxidizer staging, swirl or mixing intensity, jet momentum balance, and recirculation settings, because simulation outcomes showed that hydrogen effects on emissions, hot-spot intensity, and heating uniformity were strongly conditioned by aerodynamics and oxygen distribution. Plant retrofit programs were recommended to begin with a validated baseline digital representation of the target heat system, including high-fidelity burner near-field geometry, participating-gas radiation calibrated for water-vapor-dominant exhaust, and conjugate heat transfer through refractory and load domains, since optimization reliability depended on accurate spatial heat-flux and temperature topology. Numerical design of experiments was recommended as the standard exploration strategy, ensuring broad and balanced sampling across feasible hydrogen shares and control levels, with deliberate oversampling near stability and peak-temperature boundaries where nonlinear regime shifts occurred. Surrogate modeling was recommended as a practical accelerator for industrial decision cycles, but only when cross-validated against holdout CFD cases and when trained on datasets that preserved nonlinearity in NOx growth and uniformity degradation; conservative biasing of surrogates for safety-critical outputs such as peak wall temperature and stability margins was recommended to prevent optimistic optima. Multi-objective Pareto optimization was recommended over single-objective tuning, because efficient hydrogen operation emerged as a tradeoff surface among useful heat transfer, load-temperature uniformity, NOx index, pressure-drop penalty, and material-temperature ceilings; therefore, retrofit decisions were recommended to be expressed as operating windows rather than as single setpoints. For emissions management, strong oxidizer staging combined with recirculation-supported dilution was recommended as the first-priority control bundle at elevated hydrogen shares, with swirl and momentum tuning used to spread heat release and suppress oxygen-rich hot pockets. For product-quality protection, enhanced internal recirculation through swirl optimization and controlled jet penetration was recommended as the most direct route to restoring uniform heating under soot-free hydrogen flames. System-level recommendations included coupling furnace CFD to heat-recovery and fuel-delivery network models before finalizing targets, because hydrogen-driven changes in exhaust composition and volumetric flow affected recuperator effectiveness, regenerator cycling, and parasitic fan power; feasible hydrogen windows were recommended to be screened against these plant-scale penalties. Instrumentation recommendations included deploying heat-flux probes or infrared wall scans, exhaust oxygen and NOx analyzers, and flow metering at fuel and staging ports to keep the digital model synchronized

with operating reality and to enable periodic re-calibration. Finally, organizational recommendations stressed that hydrogen integration projects should formalize a computational-to-operational workflow in which validated models, surrogate-assisted optimization, and constraint-aware operating envelopes were updated iteratively with plant data, ensuring that efficiency improvements, emissions compliance, stability, and refractory durability were jointly maintained across real production variability.

LIMITATION

Limitations of the computational thermo-fluid dynamics modeling and optimization approach were recognized in relation to physics representation, data grounding, and generalizability across industrial contexts. First, although the Multiphysics CFD framework captured turbulent reacting flow, participating-media radiation, and conjugate heat transfer in a coupled manner, the simulations still relied on turbulence closure and turbulence–chemistry interaction models that represented complex, unsteady flame–vortex dynamics through approximations. These closures could have smoothed or displaced localized mixing structures that were especially important under hydrogen's fast chemistry, meaning that predicted hot-pocket intensity, anchoring distance, or oxygen micro-stratification may have carried model-form uncertainty beyond what integrated error statistics fully revealed. Second, radiation treatment, while hydrogen-appropriate in emphasizing water-vapor-dominated emission, still used spectral simplifications and assumed emissivity properties that were spatially averaged or weakly temperature dependent; real refractory surfaces and loads can exhibit evolving emissivity due to scale formation, oxidation, or fouling, and these shifts could have altered wall heat-flux patterns during long industrial campaigns more than the model allowed. Third, boundary conditions were parameterized from reference operating logs and pilot measurements, but several plant realities—such as unsteady fuel-header pressure fluctuations, burner wear altering jet shapes, air leakage through door seals, variable load packing density, and transient production cycling—were not explicitly represented. Those unmodeled perturbations could have narrowed stability margins or changed uniformity outcomes in practice even when the CFD operating window appeared feasible. Fourth, emissions indices were derived from resolved thermo-chemical fields under steady operating assumptions; however, industrial NOx often reflects both instantaneous peaks and time-integrated residence effects under fluctuating staging and recirculation, so transient emissions could have deviated from steady predictions. Fifth, the numerical design of experiments sampled a broad but finite space, and surrogate models learned from that space; any operating region not covered by the DOE, especially rare edge regimes involving simultaneous extreme hydrogen share and atypical staging patterns, may have been predicted less reliably even when cross-validation errors were low. Sixth, the study focused on one representative heat-system archetype at a time, so cross-sector transferability remained bounded by differences in geometry, dominant heat-transfer mode, burner technology, and production atmospheres. The indicator set enabled comparison in principle, yet sector-specific constraints—such as reducing atmospheres in certain furnaces, gas–solid coupling in kilns, or tube-metal creep limits in reformers—could have shifted optimization priorities relative to those quantified here. Seventh, system-level coupling to heat-recovery and hydrogen supply networks was represented through simplified links rather than fully dynamic co-simulation, which could have underrepresented feedbacks between exhaust variability, recuperator cycling, storage dispatch, and furnace boundary conditions. Finally, computational cost limitations restricted the degree of scale-resolving simulation that could be performed; large-eddy or fully transient campaigns across the entire DOE were not feasible, so the conclusions depended on design-level modeling assumptions typical of industrial optimization studies. These limitations did not invalidate the quantitative patterns observed, but they indicated that reported operating windows and sensitivity hierarchies should be interpreted as robust within the modeled physics and boundary realism, while still requiring careful plant-specific verification under real production variability.

REFERENCES

[1]. Abdul, H. (2023). Artificial Intelligence in Product Marketing: Transforming Customer Experience And Market Segmentation. *ASRC Procedia: Global Perspectives in Science and Scholarship*, *3*(1), 132–159. https://doi.org/10.63125/58npbx97

[2]. Abdul, H., & Mohammad Shoeb, A. (2024). The Role Of AI-Enabled Customer Segmentation In Driving Brand Performance On Online Retail Platforms. *Journal of Sustainable Development and Policy*, *3*(04), 31–64. https://doi.org/10.63125/tpjc0m87

[3]. Abdulla, M., & Md. Wahid Zaman, R. (2023). Quantitative Study On Workflow Optimization Through Data Analytics In U.S. Digital Enterprises. *American Journal of Interdisciplinary Studies*, *4*(03), 136–165. https://doi.org/10.63125/y2qshd31

[4]. Adair, D., & Jaeger, M. (2019). An efficient strategy to deliver understanding of both numerical and practical aspects when using navier-stokes equations to solve fluid mechanics problems. *Fluids*, *4*(4), 178.

[5]. Allelein, H.-J., & Verfondern, K. (2018). Major milestones of HTR development in Germany and still open research issues. *Annals of Nuclear Energy*, *116*, 114-127.

[6]. Ancona, M., Bianchi, M., Branchini, L., De Pascale, A., Melino, F., Peretto, A., Rosati, J., & Scarponi, L. (2017). From solar to hydrogen: Preliminary experimental investigation on a small scale facility. *International Journal of Hydrogen Energy*, *42*(33), 20979-20993.

[7]. Aparicio-Ruiz, R., García-González, D. L., Morales, M., Lobo-Prieto, A., & Romero, I. (2018). Comparison of two analytical methods validated for the determination of volatile compounds in virgin olive oil: GC-FID vs GC-MS. *Talanta*, *187*, 133-141.

[8]. Arfan, U., Sai Praveen, K., & Alifa Majumder, N. (2021). Predictive Analytics For Improving Financial Forecasting And Risk Management In U.S. Capital Markets. *American Journal of Interdisciplinary Studies*, *2*(04), 69–100. https://doi.org/10.63125/tbw49w69

[9]. Arfan, U., Tahsina, A., Md Mostafizur, R., & Md, W. (2023). Impact Of GFMIS-Driven Financial Transparency On Strategic Marketing Decisions In Government Agencies. *Review of Applied Science and Technology*, *2*(01), 85-112. https://doi.org/10.63125/8nqhhm56

[10]. Artinov, A., Karkhin, V., Khomich, P., Bachmann, M., & Rethmeier, M. (2019). Assessment of thermal cycles by combining thermo-fluid dynamics and heat conduction in keyhole mode welding processes. *International Journal of Thermal Sciences*, *145*, 105981.

[11]. Ayr, U., Tamborrino, A., Catalano, P., Bianchi, B., & Leone, A. (2015). 3D computational fluid dynamics simulation and experimental validation for prediction of heat transfer in a new malaxer machine. *Journal of Food Engineering*, *154*, 30-38.

[12]. Barsali, S., De Marco, A., Giglioli, R., Ludovici, G., & Possenti, A. (2015). Dynamic modelling of biomass power plant using micro gas turbine. *Renewable Energy*, *80*, 806-818.

[13]. Bellan, S., Gokon, N., Matsubara, K., Cho, H. S., & Kodama, T. (2018). Numerical and experimental study on granular flow and heat transfer characteristics of directly-irradiated fluidized bed reactor for solar gasification. *International Journal of Hydrogen Energy*, *43*(34), 16443-16457.

[14]. Berditchevskaia, A., Cazé, R., & Schultz, S. R. (2016). Performance in a GO/NOGO perceptual task reflects a balance between impulsive and instrumental components of behaviour. *Scientific reports*, *6*(1), 27389.

[15]. Broadhurst, D., Goodacre, R., Reinke, S. N., Kuligowski, J., Wilson, I. D., Lewis, M. R., & Dunn, W. B. (2018). Guidelines and considerations for the use of system suitability and quality control samples in mass spectrometry assays applied in untargeted clinical metabolomic studies. *Metabolomics*, *14*(6), 72.

[16]. Bugatti, M., & Semeraro, Q. (2018). Limitations of the inherent strain method in simulating powder bed fusion processes. *Additive Manufacturing*, *23*, 329-346.

[17]. Buonocore, J. J., Luckow, P., Norris, G., Spengler, J. D., Biewald, B., Fisher, J., & Levy, J. I. (2016). Health and climate benefits of different energy-efficiency and renewable energy choices. *Nature Climate Change*, *6*(1), 100-105.

[18]. Casella, F. (2017). Dynamic modeling and control of Organic Rankine Cycle plants. *Organic Rankine Cycle (ORC) Power Systems*, 153-171.

[19]. Catapano, F., Sementa, P., & Vaglieco, B. M. (2016). Air-fuel mixing and combustion behavior of gasoline-ethanol blends in a GDI wall-guided turbocharged multi-cylinder optical engine. *Renewable Energy*, *96*, 319-332.

[20]. Chang, C.-W., & Dinh, N. T. (2019). Classification of machine learning frameworks for data-driven thermal fluid models. *International Journal of Thermal Sciences*, *135*, 559-579.

[21]. Chen, L., Li, M., Ni, M., & Zhang, N. (2017). MHD effects and heat transfer analysis in magneto-thermo-fluid-structure coupled field in DCLL blanket. *International Communications in Heat and Mass Transfer*, *84*, 110-120.

[22]. Chen, Q., Zhai, Z., You, X., & Zhang, T. (2017). *Inverse design methods for the built environment*. Routledge.

[23]. Chen, Y., Hu, Y., & Zhang, S. (2019). Structure optimization of submerged water jet cavitating nozzle with a hybrid algorithm. *Engineering Applications of Computational Fluid Mechanics*, *13*(1), 591-608.

[24]. Cinti, G., Bidini, G., & Hemmes, K. (2019). Comparison of the solid oxide fuel cell system for micro CHP using natural gas with a system using a mixture of natural gas and hydrogen. *Applied energy*, *238*, 69-77.

[25]. Clinton, B. C., & Steinberg, D. C. (2019). Providing the Spark: Impact of financial incentives on battery electric vehicle adoption. *Journal of Environmental Economics and Management*, *98*, 102255.

[26]. Couto, N., Silva, V., Cardoso, J., González-Gutiérrez, L. M., & Souto-Iglesias, A. (2018). Coupled CFD-response surface method (RSM) methodology for optimizing jettability operating conditions. *ChemEngineering*, *2*(4), 51.

[27]. Deutschmann, O. (2015). Modeling of the interactions between catalytic surfaces and gas-phase. *Catalysis Letters*, *145*(1), 272-289.

[28]. Di Martino, G. D., Carmicino, C., Mungiguerra, S., & Savino, R. (2019). The application of computational thermo-fluid-dynamics to the simulation of hybrid rocket internal ballistics with classical or liquefying fuels: A review. *Aerospace*, *6*(5), 56.

[29]. Di Renzo, M., Zappone, A., Lam, T. T., & Debbah, M. (2018). System-level modeling and optimization of the energy efficiency in cellular networks—A stochastic geometry framework. *IEEE Transactions on Wireless Communications*, *17*(4), 2539-2556.
[30]. El Zarwi, F., Vij, A., & Walker, J. L. (2017). A discrete choice framework for modeling and forecasting the adoption and diffusion of new transportation services. *Transportation Research Part C: Emerging Technologies*, *79*, 207-223.
[31]. Enevoldsen, P., & Sovacool, B. K. (2016). Integrating power systems for remote island energy supply: Lessons from Mykines, Faroe Islands. *Renewable Energy*, *85*, 642-648.
[32]. Evangelopoulou, S., De Vita, A., Zazias, G., & Capros, P. (2019). Energy system modelling of carbon-neutral hydrogen as an enabler of sectoral integration within a decarbonization pathway. *Energies*, *12*(13), 2551.
[33]. Eveloy, V., & Gebreegziabher, T. (2018). A review of projected power-to-gas deployment scenarios. *Energies*, *11*(7), 1824.
[34]. Fang, R., & Liang, Y. (2019). Control strategy of electrolyzer in a wind-hydrogen system considering the constraints of switching times. *International Journal of Hydrogen Energy*, *44*(46), 25104-25111.
[35]. Felseghi, R.-A., Carcadea, E., Raboaca, M. S., Trufin, C. N., & Filote, C. (2019). Hydrogen fuel cell technology for the sustainable future of stationary applications. *Energies*, *12*(23), 4593.
[36]. Ferdous Ara, A. (2021). Integration Of STI Prevention Interventions Within PrEP Service Delivery: Impact On STI Rates And Antibiotic Resistance. *International Journal of Scientific Interdisciplinary Research*, *2*(2), 63–97. https://doi.org/10.63125/65143m72
[37]. Ferdous Ara, A., & Beatrice Onyinyechi, M. (2023). Long-Term Epidemiologic Trends Of STIs PRE- and POST-PrEP Introduction: A National Time-Series Analysis. *American Journal of Health and Medical Sciences*, *4*(02), 01–35. https://doi.org/10.63125/mp153d97
[38]. Figaj, R., & Vanoli, L. (2019). Hybrid and novel solar hydrogen systems. In *Solar Hydrogen Production* (pp. 487-510). Elsevier.
[39]. Fulekar, M., & Pathak, B. (2017). *Environmental nanotechnology*. CRC Press.
[40]. Gelažanskas, L., & Gamage, K. A. (2015). Forecasting hot water consumption in residential houses. *Energies*, *8*(11), 12702-12717.
[41]. Gerboni, R., & Grosso, D. (2016). Testing future hydrogen penetration at local scale through an optimisation tool. *International Journal of Hydrogen Energy*, *41*(48), 22626-22634.
[42]. Ghaffarianhoseini, A., Tookey, J., Ghaffarianhoseini, A., Naismith, N., Azhar, S., Efimova, O., & Raahemifar, K. (2017). Building Information Modelling (BIM) uptake: Clear benefits, understanding its implementation, risks and challenges. *Renewable and Sustainable Energy Reviews*, *75*, 1046-1053.
[43]. Giles, A. P., Kay, P., Mouzakitis, K., Bowen, P. J., & Crayford, A. P. (2017). On flammability hazards from pressurised high-flashpoint liquid releases. *Journal of Loss Prevention in the Process Industries*, *46*, 185-194.
[44]. Godfroid, A. (2019). *Eye tracking in second language acquisition and bilingualism: A research synthesis and methodological guide*. Routledge.
[45]. Guelpa, E., Toro, C., Sciacovelli, A., Melli, R., Sciubba, E., & Verda, V. (2016). Optimal operation of large district heating networks through fast fluid-dynamic simulation. *Energy*, *102*, 586-595.
[46]. Gyulassy, A., Bremer, P.-T., & Pascucci, V. (2018). Shared-memory parallel computation of Morse-Smale complexes with improved accuracy. *IEEE Transactions on Visualization and Computer Graphics*, *25*(1), 1183-1192.
[47]. Hamilton, C., Calusinska, M., Baptiste, S., Masset, J., Beckers, L., Thonart, P., & Hiligsmann, S. (2018). Effect of the nitrogen source on the hydrogen production metabolism and hydrogenases of Clostridium butyricum CWBI1009. *International Journal of Hydrogen Energy*, *43*(11), 5451-5462.
[48]. Han, C.-W., Jeong, S.-B., & Oh, M.-D. (2016). Thermo-fluid simulation for the thermal design of the IGBT module in the power conversion system. *Microelectronics Reliability*, *59*, 64-72.
[49]. Hari, B., Brouwer, J. P., Dhir, A., & Steinberger-Wilckens, R. (2019). A computational fluid dynamics and finite element analysis design of a microtubular solid oxide fuel cell stack for fixed wing mini unmanned aerial vehicles. *International Journal of Hydrogen Energy*, *44*(16), 8519-8532.
[50]. Heirendt, L., Arreckx, S., Pfau, T., Mendoza, S. N., Richelle, A., Heinken, A., Haraldsdóttir, H. S., Wachowiak, J., Keating, S. M., & Vlasov, V. (2019). Creation and analysis of biochemical constraint-based models using the COBRA Toolbox v. 3.0. *Nature protocols*, *14*(3), 639-702.
[51]. Hooshyari, K., Javanbakht, M., & Adibi, M. (2016). Novel composite membranes based on dicationic ionic liquid and polybenzimidazole mixtures as strategy for enhancing thermal and electrochemical properties of proton exchange membrane fuel cells applications at high temperature. *International Journal of Hydrogen Energy*, *41*(25), 10870-10883.
[52]. Hozyfa, S., & Mst. Shahrin, S. (2024). The Influence Of Secure Data Systems On Fraud Detection In Business Intelligence Applications. *Journal of Sustainable Development and Policy*, *3*(04), 133-173. https://doi.org/10.63125/8ee0eq13
[53]. Hwang, S., Kim, H., Park, J., Kwon, M.-W., Baek, M.-H., Lee, J.-J., & Park, B.-G. (2018). System-level simulation of hardware spiking neural network based on synaptic transistors and I&F neuron circuits. *IEEE Electron Device Letters*, *39*(9), 1441-1444.
[54]. Hwang, W.-K., Choy, S., Song, S. L., Lee, J., Hwang, D. S., & Lee, K.-Y. (2019). Enhancement of nanofluid stability and critical heat flux in pool boiling with nanocellulose. *Carbohydrate polymers*, *213*, 393-402.
[55]. Iervolino, G., Zammit, I., Vaiano, V., & Rizzo, L. (2019). Limitations and prospects for wastewater treatment by UV and visible-light-active heterogeneous photocatalysis: a critical review. *Heterogeneous photocatalysis: recent advances*, 225-264.

[56]. Ikäheimo, J., Kiviluoma, J., Weiss, R., & Holttinen, H. (2018). Power-to-ammonia in future North European 100% renewable power and heat system. *International Journal of Hydrogen Energy*, *43*(36), 17295-17308.
[57]. Introini, C., Lorenzi, S., Cammi, A., Baroli, D., Peters, B., & Bordas, S. (2018). A mass conservative Kalman filter algorithm for computational thermo-fluid dynamics. *Materials*, *11*(11), 2222.
[58]. Ishaq, H., & Dincer, I. (2019). Design and performance evaluation of a new biomass and solar based combined system with thermochemical hydrogen production. *Energy Conversion and Management*, *196*, 395-409.
[59]. Jabed Hasan, T., & Mohammad Shah, P. (2024). Quantitative Assessment Of Automation And Control Strategies For Performance Optimization In U.S. Industrial Plants. *ASRC Procedia: Global Perspectives in Science and Scholarship*, *4*(1), 169–205. https://doi.org/10.63125/eqfz8220
[60]. Jabed Hasan, T., & Zayadul, H. (2024). Adapting PLC/SCADA Systems To Mitigate Industrial IOT Cybersecurity Risks In Global Manufacturing. *American Journal of Interdisciplinary Studies*, *5*(04), 67-95. https://doi.org/10.63125/0v4cms60
[61]. Jahid, M. K. A. S. R. (2021). Digital Transformation Frameworks For Smart Real Estate Development In Emerging Economies. *Review of Applied Science and Technology*, *6*(1), 139–182. https://doi.org/10.63125/cd09ne09
[62]. James, K. L., Randall, N. P., & Haddaway, N. R. (2016). A methodology for systematic mapping in environmental sciences. *Environmental evidence*, *5*(1), 7.
[63]. James, M. R., Robson, S., d'Oleire-Oltmanns, S., & Niethammer, U. (2017). Optimising UAV topographic surveys processed with structure-from-motion: Ground control quality, quantity and bundle adjustment. *Geomorphology*, *280*, 51-66.
[64]. Jao, C.-K., Wang, C.-Y., Yeh, T.-Y., Tsai, C.-C., Lo, L.-C., Chen, J.-H., Pao, W.-C., & Sheen, W.-H. (2018). WiSE: A system-level simulator for 5G mobile networks. *IEEE Wireless Communications*, *25*(2), 4-7.
[65]. Jiang, B., Santis-Alvarez, A. J., Muralt, P., Poulikakos, D., Borhani, N., Thome, J. R., & Maeder, T. (2015). Design and packaging of a highly integrated microreactor system for high-temperature on-board hydrogen production. *Chemical Engineering Journal*, *275*, 206-219.
[66]. Kabeel, A., El-Said, E. M., & Abdulaziz, M. (2019). Computational fluid dynamic as a tool for solar still performance analysis and design development: a review. *Desalination and Water Treatment*, *159*, 200-213.
[67]. Kalnay, E., Kanamitsu, M., Kistler, R., Collins, W., Deaven, D., Gandin, L., Iredell, M., Saha, S., White, G., & Woollen, J. (2018). The NCEP/NCAR 40-year reanalysis project. In *Renewable Energy* (pp. Vol1_146-Vol141_194). Routledge.
[68]. Ksouri, I., & Haddar, N. (2018). Long term ageing of polyamide 6 and polyamide 6 reinforced with 30% of glass fibers: temperature effect. *Journal of Polymer Research*, *25*(7), 153.
[69]. Kubli, M., & Ulli-Beer, S. (2016). Decentralisation dynamics in energy systems: A generic simulation of network effects. *Energy Research & Social Science*, *13*, 71-83.
[70]. Kurşun, B., & Ökten, K. (2019). Thermodynamic analysis of a Rankine cycle coupled with a concentrated photovoltaic thermal system for hydrogen production by a proton exchange membrane electrolyzer plant. *International Journal of Hydrogen Energy*, *44*(41), 22863-22875.
[71]. Lachman, R., Lachman, J. L., & Butterfield, E. C. (2015). *Cognitive psychology and information processing: An introduction*. Psychology Press.
[72]. Lamnatou, C., Mondol, J. D., Chemisana, D., & Maurer, C. (2015). Modelling and simulation of Building-Integrated solar thermal systems: Behaviour of the system. *Renewable and Sustainable Energy Reviews*, *45*, 36-51.
[73]. Landoulsi, J., Genet, M. J., Fleith, S., Touré, Y., Liascukiene, I., Méthivier, C., & Rouxhet, P. G. (2016). Organic adlayer on inorganic materials: XPS analysis selectivity to cope with adventitious contamination. *Applied Surface Science*, *383*, 71-83.
[74]. Leblebici, A., Mayor, P., Rajman, M., & De Micheli, G. (2018). Smart Energy. In *Nano-Tera. ch: Engineering the Future of Systems for Health, Environment and Energy* (pp. 109-137). Springer.
[75]. Li, A., Song, C., & Lin, Z. (2017). A multiphysics fully coupled modeling tool for the design and operation analysis of planar solid oxide fuel cell stacks. *Applied energy*, *190*, 1234-1244.
[76]. Li, M., Xu, J., Xie, H., & Wang, Y. (2018). Transport biofuels technological paradigm based conversion approaches towards a bio-electric energy framework. *Energy Conversion and Management*, *172*, 554-566.
[77]. Liu, C., & Lin, Z. (2017). How uncertain is the future of electric vehicle market: Results from Monte Carlo simulations using a nested logit model. *International Journal of Sustainable Transportation*, *11*(4), 237-247.
[78]. Liu, Q., & Brown, D. (2015). Methodological synthesis of research on the effectiveness of corrective feedback in L2 writing. *Journal of Second Language Writing*, *30*, 66-81.
[79]. Liu, W., & Chen, Q. (2015). Optimal air distribution design in enclosed spaces using an adjoint method. *Inverse Problems in Science and Engineering*, *23*(5), 760-779.
[80]. Liu, W., Jin, M., Chen, C., & Chen, Q. (2016). Optimization of air supply location, size, and parameters in enclosed environments using a computational fluid dynamics-based adjoint method. *Journal of Building Performance Simulation*, *9*(2), 149-161.
[81]. Magdeldin, M., Kohl, T., De Blasio, C., Järvinen, M., Won Park, S., & Giudici, R. (2016). The BioSCWG project: Understanding the trade-offs in the process and thermal design of hydrogen and synthetic natural gas production. *Energies*, *9*(10), 838.
[82]. Magliocca, N. R., Rudel, T. K., Verburg, P. H., McConnell, W. J., Mertz, O., Gerstner, K., Heinimann, A., & Ellis, E. C. (2015). Synthesis in land change science: methodological patterns, challenges, and guidelines. *Regional environmental change*, *15*(2), 211-226.

[83]. Malerød-Fjeld, H., Clark, D., Yuste-Tirados, I., Zanón, R., Catalán-Martinez, D., Beeaff, D., Morejudo, S. H., Vestre, P. K., Norby, T., & Haugsrud, R. (2017). Thermo-electrochemical production of compressed hydrogen from methane with near-zero energy loss. *Nature Energy*, *2*(12), 923-931.

[84]. Marshall, C. R., Howrigan, D. P., Merico, D., Thiruvahindrapuram, B., Wu, W., Greer, D. S., Antaki, D., Shetty, A., Holmans, P. A., & Pinto, D. (2017). Contribution of copy number variants to schizophrenia from a genome-wide study of 41,321 subjects. *Nature genetics*, *49*(1), 27-35.

[85]. Matinheikki, J., Pesonen, T., Artto, K., & Peltokorpi, A. (2017). New value creation in business networks: The role of collective action in constructing system-level goals. *Industrial Marketing Management*, *67*, 122-133.

[86]. Maxwell, S. E., Delaney, H. D., & Kelley, K. (2017). *Designing experiments and analyzing data: A model comparison perspective*. Routledge.

[87]. Md Al Amin, K., & Md Mesbaul, H. (2023). Smart Hybrid Manufacturing: A Combination Of Additive, Subtractive, And Lean Techniques For Agile Production Systems. *Journal of Sustainable Development and Policy*, *2*(04), 174-217. https://doi.org/10.63125/7rb1zz78

[88]. Md Ariful, I., & Efat Ara, H. (2022). Advances And Limitations Of Fracture Mechanics–Based Fatigue Life Prediction Approaches For Structural Integrity Assessment: A Systematic Review. *American Journal of Interdisciplinary Studies*, *3*(03), 68-98. https://doi.org/10.63125/fg8ae957

[89]. Md Arman, H., & Md.Kamrul, K. (2022). A Systematic Review of Data-Driven Business Process Reengineering And Its Impact On Accuracy And Efficiency Corporate Financial Reporting. *International Journal of Business and Economics Insights*, *2*(4), 01–41. https://doi.org/10.63125/btx52a36

[90]. Md Foysal, H., & Aditya, D. (2023). Smart Continuous Improvement With Artificial Intelligence, Big Data, And Lean Tools For Zero Defect Manufacturing Systems. *American Journal of Scholarly Research and Innovation*, *2*(01), 254–282. https://doi.org/10.63125/6cak0s21

[91]. Md Hamidur, R. (2023). Thermal & Electrical Performance Enhancement Of Power Distribution Transformers In Smart Grids. *American Journal of Scholarly Research and Innovation*, *2*(01), 283–313. https://doi.org/10.63125/n2p6y628

[92]. Md Harun-Or-Rashid, M., Mst. Shahrin, S., & Sai Praveen, K. (2023). Integration Of IOT And EDGE Computing For Low-Latency Data Analytics In Smart Cities And IOT Networks. *Journal of Sustainable Development and Policy*, *2*(03), 01-33. https://doi.org/10.63125/004h7m29

[93]. Md Mesbaul, H., & Md. Tahmid Farabe, S. (2022). Implementing Sustainable Supply Chain Practices In Global Apparel Retail: A Systematic Review Of Current Trends. *ASRC Procedia: Global Perspectives in Science and Scholarship*, *2*(1), 332–363. https://doi.org/10.63125/nen7vd57

[94]. Md Musfiqur, R., & Md.Kamrul, K. (2023). Mechanisms By Which AI-Enabled Crm Systems Influence Customer Retention And Overall Business Performance: A Systematic Literature Review Of Empirical Findings. *International Journal of Business and Economics Insights*, *3*(1), 31-67. https://doi.org/10.63125/qqe2bm11

[95]. Md Muzahidul, I., & Aditya, D. (2024). Predictive Analytics And Data-Driven Algorithms For Improving Efficiency In Full-Stack Web Systems. *International Journal of Scientific Interdisciplinary Research*, *5*(2), 226–260. https://doi.org/10.63125/q75tbj05

[96]. Md Muzahidul, I., & Md Mohaiminul, H. (2023). Explainable AI (XAI) Models For Cloud-Based Business Intelligence: Ensuring Compliance And Secure Decision-Making. *American Journal of Interdisciplinary Studies*, *4*(03), 208–249. https://doi.org/10.63125/5etfhh77

[97]. Md Nahid, H. (2022). Statistical Analysis of Cyber Risk Exposure And Fraud Detection In Cloud-Based Banking Ecosystems. *ASRC Procedia: Global Perspectives in Science and Scholarship*, *2*(1), 289–331. https://doi.org/10.63125/9wf91068

[98]. Md Sarwar Hossain, S., & Md Milon, M. (2022). Machine Learning-Based Pavement Condition Prediction Models For Sustainable Transportation Systems. *American Journal of Interdisciplinary Studies*, *3*(01), 31–64. https://doi.org/10.63125/1jsmkg92

[99]. Md. Abdur, R., & Zamal Haider, S. (2022). Assessment Of Data-Driven Vendor Performance Evaluation In Retail Supply Chains Analyzing Metrics, Scorecards, And Contract Management Tools. *Journal of Sustainable Development and Policy*, *1*(04), 71-116. https://doi.org/10.63125/2a641k35

[100]. Md. Al Amin, K., & Sai Praveen, K. (2023). The Role Of Industrial Engineering In Advancing Sustainable Manufacturing And Quality Compliance In Global Engineering Systems. *International Journal of Scientific Interdisciplinary Research*, *4*(4), 31–61. https://doi.org/10.63125/8w1vk676

[101]. Md. Hasan, I., & Ashraful, I. (2023). The Effect Of Production Planning Efficiency On Delivery Timelines In U.S. Apparel Imports. *Journal of Sustainable Development and Policy*, *2*(04), 35-73. https://doi.org/10.63125/sg472m51

[102]. Md. Hasan, I., & Rakibul, H. (2024). Quantitative Assessment Of Compliance And Inspection Practices In Reducing Supply Chain Disruptions. *International Journal of Scientific Interdisciplinary Research*, *5*(2), 301–342. https://doi.org/10.63125/db63r616

[103]. Md. Mominul, H. (2024). Quantitative Assessment Of Smart City IOT Integration For Reducing Urban Infrastructure Vulnerabilities. *Review of Applied Science and Technology*, *3*(04), 48-93. https://doi.org/10.63125/f2cj4507

[104]. Md. Mominul, H., & Syed Zaki, U. (2024). A Review On Sustainable Building Materials And Their Role In Enhancing U.S. Green Infrastructure Goals. *Journal of Sustainable Development and Policy*, *3*(04), 65-100. https://doi.org/10.63125/bfmmay79

[105]. Md.Akbar, H., & Farzana, A. (2021). High-Performance Computing Models For Population-Level Mental Health Epidemiology And Resilience Forecasting. *American Journal of Health and Medical Sciences*, *2*(02), 01–33. https://doi.org/10.63125/k9d5h638

[106]. Meisl, G., Kirkegaard, J. B., Arosio, P., Michaels, T. C., Vendruscolo, M., Dobson, C. M., Linse, S., & Knowles, T. P. (2016). Molecular mechanisms of protein aggregation from global fitting of kinetic models. *Nature protocols*, *11*(2), 252-272.

[107]. Mejdoub, H., & Ghorbel, A. (2018). Conditional dependence between oil price and stock prices of renewable energy: A vine copula approach. *Economic and Political Studies*, *6*(2), 176-193.

[108]. Messig, D., Vascellari, M., & Hasse, C. (2017). Flame structure analysis and flamelet progress variable modelling of strained coal flames. *Combustion Theory and Modelling*, *21*(4), 700-721.

[109]. Meyers, R. M., Bryan, J. G., McFarland, J. M., Weir, B. A., Sizemore, A. E., Xu, H., Dharia, N. V., Montgomery, P. G., Cowley, G. S., & Pantel, S. (2017). Computational correction of copy number effect improves specificity of CRISPR–Cas9 essentiality screens in cancer cells. *Nature genetics*, *49*(12), 1779-1784.

[110]. Milani, M., Montorsi, L., Stefani, M., Saponelli, R., & Lizzano, M. (2017). Numerical analysis of an entire ceramic kiln under actual operating conditions for the energy efficiency improvement. *Journal of environmental management*, *203*, 1026-1037.

[111]. Milani, M., Montorsi, L., Venturelli, M., Tiscar, J., & García-Ten, J. (2019). A numerical approach for the combined analysis of the dynamic thermal behaviour of an entire ceramic roller kiln and the stress formation in the tiles. *Energy*, *177*, 543-553.

[112]. Minotti, A., & Teofilatto, P. (2015). Swirling combustor energy converter: H2/Air simulations of separated chambers. *Energies*, *8*(9), 9930-9945.

[113]. Mohammad Mushfequr, R., & Ashraful, I. (2023). Automation And Risk Mitigation in Healthcare Claims: Policy And Compliance Implications. *Review of Applied Science and Technology*, *2*(04), 124–157. https://doi.org/10.63125/v73gyg14

[114]. Mohammad Mushfequr, R., & Sai Praveen, K. (2022). Quantitative Investigation Of Information Security Challenges In U.S. Healthcare Payment Ecosystems. *International Journal of Business and Economics Insights*, *2*(4), 42–73. https://doi.org/10.63125/gcg0fs06

[115]. Mortuza, M. M. G., & Rauf, M. A. (2022). Industry 4.0: An Empirical Analysis of Sustainable Business Performance Model Of Bangladeshi Electronic Organisations. *International Journal of Economy and Innovation*. https://gospodarkainnowacje.pl/index.php/issue_view_32/article/view/826

[116]. Motasemi, F., & Gerber, A. (2018). Multicomponent conjugate heat and mass transfer in biomass materials during microwave pyrolysis for biofuel production. *Fuel*, *211*, 649-660.

[117]. Namugenyi, C., Nimmagadda, S. L., & Reiners, T. (2019). Design of a SWOT analysis model and its evaluation in diverse digital business ecosystem contexts. *Procedia Computer Science*, *159*, 1145-1154.

[118]. O'Brien, K. K., Colquhoun, H., Levac, D., Baxter, L., Tricco, A. C., Straus, S., Wickerson, L., Nayar, A., Moher, D., & O'Malley, L. (2016). Advancing scoping study methodology: a web-based survey and consultation of perceptions on terminology, definition and methodological steps. *BMC health services research*, *16*(1), 305.

[119]. Pankaz Roy, S., & Md. Kamrul, K. (2023). HACCP and ISO Frameworks For Enhancing Biosecurity In Global Food Distribution Chains. *American Journal of Scholarly Research and Innovation*, *2*(01), 314–356. https://doi.org/10.63125/9pbp4h37

[120]. Pankaz Roy, S., & Sai Praveen, K. (2024). Systematic Review of Stress And Burnout Interventions Among U.S. Healthcare Professionals Using Advanced Computing Approaches. *Journal of Sustainable Development and Policy*, *3*(04), 101-132. https://doi.org/10.63125/9mx2fc43

[121]. Papasidero, D., Pierucci, S., Manenti, F., & Piazza, L. (2017). A General Model for Food Cooking Undergoing Phase Changes. In *The Water-Food-Energy Nexus* (pp. 249-273). CRC Press.

[122]. Patella, S., Scrucca, F., Asdrubali, F., & Carrese, S. (2019). Carbon Footprint of autonomous vehicles at the urban mobility system level: A traffic simulation-based approach. *Transportation Research Part D: Transport and Environment*, *74*, 189-200.

[123]. Peksen, M. (2015). 3D CFD/FEM analysis of thermomechanical long-term behaviour in SOFCs: Furnace operation with different fuel gases. *International Journal of Hydrogen Energy*, *40*(36), 12362-12369.

[124]. Pettinau, A., Calì, G., Loria, E., Miraglia, P., & Ferrara, F. (2015). The Sotacarbo gasification pilot platform: Plant overview, recent experimental results and potential future integrations. *Applied Thermal Engineering*, *74*, 2-9.

[125]. Qu, Z., Shi, H., Yu, X., Wang, Q., & Ma, T. (2019). Optimization of thermoelectric generator integrated recuperator. *Energy Procedia*, *158*, 2058-2063.

[126]. Rahman, M. H., Uddinb, M. K. S., Hossanc, K. M. R., & Hossaind, M. D. (2024). The role of predictive analytics in early disease detection: a data-driven approach to preventive healthcare. *Journal of the Learning Sciences*, *32*(2), 2024.

[127]. Rakibul, H., & Samia, A. (2022). Information System-Based Decision Support Tools: A Systematic Review Of Strategic Applications In Service-Oriented Enterprises. *Review of Applied Science and Technology*, *1*(04), 26-65. https://doi.org/10.63125/w3cevz78

[128]. Raven, R., Ghosh, B., Wieczorek, A., Stirling, A., Ghosh, D., Jolly, S., Karjangtimapron, E., Prabudhanitisarn, S., Roy, J., & Sangawongse, S. (2017). Unpacking sustainabilities in diverse transition contexts: solar photovoltaic and urban mobility experiments in India and Thailand. *Sustainability Science*, *12*(4), 579-596.

[129]. Reza, M., Vorobyova, K., & Rauf, M. (2021). The effect of total rewards system on the performance of employees with a moderating effect of psychological empowerment and the mediation of motivation in the leather industry of Bangladesh. *Engineering Letters*, *29*, 1-29.

[130]. Rodriguez, G. R., Garelli, L., Storti, M., Granata, D., Amadei, M., & Rossetti, M. (2017). Numerical and experimental thermo-fluid dynamic analysis of a power transformer working in ONAN mode. *Applied Thermal Engineering*, *112*, 1271-1280.

[131]. Rony, M. A., & Ashraful, I. (2022). Big Data And Engineering Analytics Pipelines For Smart Manufacturing: Enhancing Efficiency, Quality, And Predictive Maintenance. *American Journal of Scholarly Research and Innovation*, *1*(02), 59–85. https://doi.org/10.63125/rze0my79

[132]. Rony, M. A., & Hozyfa, S. (2024). Cloud-Integrated Digital Twin Architectures For Real-Time Monitoring, Risk Assessment, And Safety Optimization In U.S. Energy Infrastructure. *American Journal of Interdisciplinary Studies*, *5*(04), 96-133. https://doi.org/10.63125/y9m5pz24

[133]. Rosen, M. A., & Koohi-Fayegh, S. (2016). The prospects for hydrogen as an energy carrier: an overview of hydrogen energy and hydrogen energy systems. *Energy, Ecology and Environment*, *1*(1), 10-29.

[134]. Rosique, F., Navarro, P. J., Fernández, C., & Padilla, A. (2019). A systematic review of perception system and simulators for autonomous vehicles research. *Sensors*, *19*(3), 648.

[135]. Rossignoli, F., & Lionzo, A. (2018). Network impact on business models for sustainability: Case study in the energy sector. *Journal of cleaner production*, *182*, 694-704.

[136]. Rzehak, R. (2016). Euler-Euler modeling of poly-dispersed bubbly flows. In *Handbook of Multiphase Flow Science and Technology* (pp. 1-37). Springer.

[137]. Saba, A., & Md. Sakib Hasan, H. (2024). Machine Learning And Secure Data Pipelines For Enhancing Patient Safety In Electronic Health Record (EHR) Among U.S. Healthcare Providers. *ASRC Procedia: Global Perspectives in Science and Scholarship*, *4*(1), 124–168. https://doi.org/10.63125/qm4he747

[138]. Saba, A., Shaikat, B., & Tonoy Kanti, C. (2023). Integration Of Artificial Intelligence And Advanced Computing To Develop Resilient Cyber Defense Systems. *Journal of Sustainable Development and Policy*, *2*(04), 74-107. https://doi.org/10.63125/rxyc6y88

[139]. Saba, A., & Tonoy Kanti, C. (2023). Explainable Artificial Intelligence (XAI) Approaches For Cyber Risk Assessment In Financial Services. *American Journal of Interdisciplinary Studies*, *4*(03), 96-135. https://doi.org/10.63125/3gjcb322

[140]. Saikat, S. (2021). Real-Time Fault Detection in Industrial Assets Using Advanced Vibration Dynamics And Stress Analysis Modeling. *American Journal of Interdisciplinary Studies*, *2*(04), 39–68. https://doi.org/10.63125/0h163429

[141]. Saikat, S. (2022). CFD-Based Investigation of Heat Transfer Efficiency In Renewable Energy Systems. *International Journal of Scientific Interdisciplinary Research*, *1*(01), 129–162. https://doi.org/10.63125/ttw40456

[142]. Santamouris, M. (2017). Passive cooling of buildings. In *Advances in Solar Energy: Volume 16* (pp. 295-344). Routledge.

[143]. Scafati, F. T., Lavorgna, M., Mancaruso, E., & Vaglieco, B. M. (2018). Nonlinear Systems and Circuits in Internal Combustion Engines Modeling and Control.

[144]. Shaikat, B., & Md. Wahid Zaman, R. (2024). Quantum-Resistant Cryptographic Protocols Integrated With AI For Securing Cloud And IOT Environments. *International Journal of Business and Economics Insights*, *4*(4), 60–90. https://doi.org/10.63125/dryw3b96

[145]. Shaikh, S., & Aditya, D. (2021). Federated Learning-Driven Predictive Quality Analytics and Supply Chain Optimization In Distributed Manufacturing Networks. *Review of Applied Science and Technology*, *6*(1), 74-107. https://doi.org/10.63125/k18cbz55

[146]. Shaikh, S., & Md. Tahmid Farabe, S. (2023). Digital Twin-Driven Process Modeling For Energy Efficiency And Lifecycle Optimization In Industrial Facilities. *American Journal of Interdisciplinary Studies*, *4*(03), 65–95. https://doi.org/10.63125/e4q64869

[147]. Snilstveit, B., Vojtkova, M., Bhavsar, A., Stevenson, J., & Gaarder, M. (2016). Evidence & Gap Maps: A tool for promoting evidence informed policy and strategic research agendas. *Journal of Clinical Epidemiology*, *79*, 120-129.

[148]. Sorgulu, F., & Dincer, I. (2018). A renewable source based hydrogen energy system for residential applications. *International Journal of Hydrogen Energy*, *43*(11), 5842-5851.

[149]. Soyez, J.-B., Morvan, G., Merzouki, R., & Dupont, D. (2015). Multilevel agent-based modeling of system of systems. *IEEE Systems Journal*, *11*(4), 2084-2095.

[150]. Speirs, J., Balcombe, P., Johnson, E., Martin, J., Brandon, N., & Hawkes, A. (2018). A greener gas grid: What are the options. *Energy Policy*, *118*, 291-297.

[151]. Stamatakis, E., Yiotis, A., Giannissi, S., Tolias, I., & Stubos, A. (2018). Modeling and simulation supporting the application of fuel cell & hydrogen technologies. *Journal of computational science*, *27*, 10-20.

[152]. Sudipto, R., & Md. Hasan, I. (2024). Data-Driven Supply Chain Resilience Modeling Through Stochastic Simulation And Sustainable Resource Allocation Analytics. *American Journal of Advanced Technology and Engineering Solutions*, *4*(02), 01-32. https://doi.org/10.63125/p0ptag78

[153]. Sun, X.-Y., Ma, S., Li, M., & Gao, L. (2017). Thermo-fluid simulation of the advanced IGBT module in a power stack. 2017 18th International Conference on Electronic Packaging Technology (ICEPT),

[154]. Tagliavini, G., Defraeye, T., & Carmeliet, J. (2019). Multiphysics modeling of convective cooling of non-spherical, multi-material fruit to unveil its quality evolution throughout the cold chain. *Food and Bioproducts Processing*, *117*, 310-320.

[155]. Teschendorff, A. E., & Relton, C. L. (2018). Statistical and integrative system-level analysis of DNA methylation data. *Nature Reviews Genetics*, *19*(3), 129-147.

[156]. Teslyuk, T., Tsmots, I., Teslyuk, V., Medykovskyy, M., & Opotyak, Y. (2017). Architecture and models for system-level computer-aided design of the management system of energy efficiency of technological processes at the enterprise. Conference on Computer Science and Information Technologies,

[157]. Thybring, E. E., Kymäläinen, M., & Rautkari, L. (2018). Experimental techniques for characterising water in wood covering the range from dry to fully water-saturated. *Wood Science and Technology*, *52*(2), 297-329.
[158]. Tonoy Kanti, C., & Saba, A. (2024). High-Performance Computing Architectures To Strengthen Cloud Infrastructure Security. *American Journal of Interdisciplinary Studies*, *5*(03), 01–42. https://doi.org/10.63125/9hr8qk06
[159]. Tonoy Kanti, C., & Sai Praveen, K. (2024). Federated Learning Models for Privacy-Preserving Data Sharing And Secure Analytics In Healthcare Industry. *International Journal of Business and Economics Insights*, *4*(4), 91-133. https://doi.org/10.63125/c2dzn006
[160]. Tonoy Kanti, C., & Shaikat, B. (2021). Blockchain-Enabled Security Protocols Combined With AI For Securing Next-Generation Internet Of Things (IOT) Networks. *International Journal of Scientific Interdisciplinary Research*, *2*(2), 98–127. https://doi.org/10.63125/pcdqzw41
[161]. Tricco, A. C., Antony, J., Soobiah, C., Kastner, M., MacDonald, H., Cogo, E., Lillie, E., Tran, J., & Straus, S. E. (2016). Knowledge synthesis methods for integrating qualitative and quantitative data: a scoping review reveals poor operationalization of the methodological steps. *Journal of Clinical Epidemiology*, *73*, 29-35.
[162]. Tricco, A. C., Lillie, E., Zarin, W., O'brien, K., Colquhoun, H., Kastner, M., Levac, D., Ng, C., Sharpe, J. P., & Wilson, K. (2016). A scoping review on the conduct and reporting of scoping reviews. *BMC medical research methodology*, *16*(1), 15.
[163]. Tricco, A. C., Soobiah, C., Antony, J., Cogo, E., MacDonald, H., Lillie, E., Tran, J., D'Souza, J., Hui, W., & Perrier, L. (2016). A scoping review identifies multiple emerging knowledge synthesis methods, but few studies operationalize the method. *Journal of Clinical Epidemiology*, *73*, 19-28.
[164]. Vogel, F. (2019). Hydrothermal conversion of biomass. In *Energy from Organic Materials (Biomass)* (pp. 1251-1295). Springer.
[165]. Wang, T., Chen, Y., Qiao, M., & Snoussi, H. (2018). A fast and robust convolutional neural network-based defect detection model in product quality control. *The International Journal of Advanced Manufacturing Technology*, *94*(9), 3465-3471.
[166]. Yu, P., Ma, W., Villanueva, W., Karbojian, A., & Bechta, S. (2019). Validation of a thermo-fluid-structure coupling approach for RPV creep failure analysis against FOREVER-EC2 experiment. *Annals of Nuclear Energy*, *133*, 637-648.
[167]. Zamal Haider, S., & Hozyfa, S. (2023). A Quantitative Study On IT-Enabled ERP Systems And Their Role In Operational Efficiency. *International Journal of Scientific Interdisciplinary Research*, *4*(4), 62–99. https://doi.org/10.63125/nbpyce10
[168]. Zamal Haider, S., & Sai Praveen, K. (2024). Cloud-Native Data Pipelines For Scalable Audio Analytics And Secure Enterprise Applications. *American Journal of Scholarly Research and Innovation*, *3*(01), 52-83. https://doi.org/10.63125/m4f2aw73
[169]. Zhang, M., Gou, W., Li, L., Wang, X., & Yue, Z. (2016). Multidisciplinary design and optimization of the twin-web turbine disk. *Structural and Multidisciplinary Optimization*, *53*(5), 1129-1141.
[170]. Zhao, G., Nielsen, E. R., Troncoso, E., Hyde, K., Romeo, J. S., & Diderich, M. (2019). Life cycle cost analysis: A case study of hydrogen energy application on the Orkney Islands. *International Journal of Hydrogen Energy*, *44*(19), 9517-9528.
[171]. Zheng, P., Wang, H., Sang, Z., Zhong, R. Y., Liu, Y., Liu, C., Mubarok, K., Yu, S., & Xu, X. (2018). Smart manufacturing systems for Industry 4.0: Conceptual framework, scenarios, and future perspectives. *Frontiers of Mechanical Engineering*, *13*(2), 137-150.
[172]. Zheng, Z., Xu, Y., & He, Y. (2016). Thermal analysis of a solar parabolic trough receiver tube with porous insert optimized by coupling genetic algorithm and CFD. *Science China Technological Sciences*, *59*(10), 1475-1485.
[173]. Zhou, W., Nielsen, J. B., Fritsche, L. G., Dey, R., Gabrielsen, M. E., Wolford, B. N., LeFaive, J., VandeHaar, P., Gagliano, S. A., & Gifford, A. (2018). Efficiently controlling for case-control imbalance and sample relatedness in large-scale genetic association studies. *Nature genetics*, *50*(9), 1335-1341.
[174]. Zhu, W., Shi, J., & Abdelwahed, S. (2018). End-to-end system level modeling and simulation for medium-voltage DC electric ship power systems. *International Journal of Naval Architecture and Ocean Engineering*, *10*(1), 37-47.
[175]. Zobayer, E. (2021a). Data Driven Predictive Maintenance In Petroleum And Power Systems Using Random Forest Regression Model For Reliability Engineering Framework. *Review of Applied Science and Technology*, *6*(1), 108-138. https://doi.org/10.63125/5bjx6963
[176]. Zobayer, E. (2021b). Machine Learning Approaches For Optimization Of Lubricant Performance And Reliability In Complex Mechanical And Manufacturing Systems. *American Journal of Scholarly Research and Innovation*, *1*(01), 61–92. https://doi.org/10.63125/5zvkgg52
[177]. Zobayer, E. (2023). IOT Integration In Intelligent Lubrication Systems For Predictive Maintenance And Performance Optimization In Advanced Manufacturing Industries. *Journal of Sustainable Development and Policy*, *2*(04), 140-173. https://doi.org/10.63125/zybrmx69
[178]. Zobayer, E., & Sabuj Kumar, S. (2024). Enhancing HFO Separator Efficiency: A Data-Driven Approach To Petroleum Systems Optimization. *International Journal of Scientific Interdisciplinary Research*, *5*(2), 261–300. https://doi.org/10.63125/2tzaap28
[179]. Zulqarnain, F. N. U., & Zayadul, H. (2024). Artificial Intelligence Applications For Predicting Renewable-Energy Demand Under Climate Variability. *American Journal of Scholarly Research and Innovation*, *3*(01), 84–116. https://doi.org/10.63125/sg0j6930